

A pollen-based reconstruction of the paleoenvironment
and cultural landscape in Southeastern Norway from the
Iron Age to the Middle Ages



Anna de Bode

Figure 1: Sampling for radiocarbon dating, Haraldstadmyr peat sequence, 2021.

A pollen-based reconstruction of the paleoenvironment and cultural landscape in Southeastern Norway from the Iron Age to the Middle Ages

Anna de Bode, s2104385

Thesis BA3, 1083VBTHEY

Supervised by Dr. J.A. Mol (University of Leiden)

Co-supervised by Prof. Dr. F. Iversen, and Prof. Dr. K. Krüger (University of Oslo); Prof. Dr. C.C. Bakels (University of Leiden); Dr. M.J.A. Bajard and E. G. Ballo (University of Oslo)

a.b.g.de.bode@vuw.leidenuniv.nl

University of Leiden, Faculty of Archaeology

Oslo, 15 June 2021, final version

Table of Contents

1. Introduction	7
1.1 <i>Past landscape utilization in Norway</i>	7
1.2 <i>Research questions</i>	9
1.3 <i>Outline of the thesis</i>	10
1.4 <i>Settings and background of the study</i>	11
1.4.1 The study site	11
1.4.2 Geology of the area	15
1.4.3 Vegetation of the area	16
1.4.4 Farming in the area	18
1.4.5 Bjørnstad burial site	19
1.5 <i>The formation of peat bogs</i>	19
1.6 <i>Pollen as a proxy</i>	22
1.7 <i>Anthropogenic indicators</i>	22
1.8 <i>Production, dispersal, deposition and preservation of pollen</i>	24
2. Methods	27
2.1 <i>Introduction</i>	27
2.2 <i>Sampling</i>	27
2.3 <i>Chronology</i>	28
2.4 <i>Pollen analysis</i>	29
2.5 <i>Pollen diagrams</i>	29
2.5.1 The input data	29
2.5.2 Construction of the pollen diagrams in R-ríoja	31
2.6 <i>Archaeological data</i>	33
3. Chronology	34
3.1 <i>Lithology</i>	34
3.2 <i>Age-depth model</i>	37
4. Pollen record	39
4.1 <i>Local vegetation</i>	39
4.2 <i>Regional vegetation</i>	40

5. Archaeological data	47
5.1 <i>Finds in the area</i>	47
5.2 <i>Burials along the Raet in Vestfold district</i>	47
5.3 <i>Burials along the Raet in Østfold district</i>	48
5.4 <i>Radiocarbon dates from Bjørnstad burial site</i>	48
6. Discussion	56
6.1 <i>Development of the local vegetation and environment of Haraldstadmyr bog</i>	56
6.2 <i>Development of the regional vegetation and environment</i>	58
6.3 <i>Evolution of farming activities from the Early Iron Age to the Medieval Period</i>	59
6.3.1 <i>A new onset of farming in the Early Iron Age</i>	59
6.3.2 <i>Transitions from pastoral to mixed farming from the Late Iron Age into the Viking Age</i>	60
6.3.3 <i>Abandonment in the Late Viking Age into the Early Middle Ages</i>	62
6.4 <i>Forcing factors of transitions in the pollen record</i>	66
6.5 <i>Reliability and limitations of the study</i>	68
7. Conclusion	70
7.1 <i>Summary and conclusions</i>	70
7.2 <i>Further research</i>	73
8. Figures, tables and appendices	80
8.1 <i>Figures</i>	80
8.3 <i>Tables</i>	80
8.4 <i>Appendices</i>	81

Acknowledgements

This thesis was written as a part of the VIKINGS project¹ at the University of Oslo. The opportunity to participate this project has been an extremely valuable experience for me. First and foremost, I would like to thank my main supervisor Dr. J. A. Mol. I want to express my deepest appreciation for encouraging and challenging me throughout the duration of this project and for giving me the opportunity to write my thesis based at the VIKINGS project in Oslo. Thank you for all your patience; inspiring meetings and for always making the time to set me on the right track.

I want to express my gratitude to my co-supervisor Prof. Dr. F. Iversen. Thank you for all your valuable ideas, your enthusiasm, the outstanding opportunities you have giving me and for providing the Norwegian literature that I would never have found myself. I want to extend my deepest gratitude to my co-supervisor Prof. Dr. K. Krüger. Thank you for inspiring me to think critically; for including me in the VIKINGS project; for all the weekly meetings and valuable opportunities to present, participate and learn. It has been an amazing year and a wonderful journey. I'm extremely grateful for all your enthusiasm, positivity and support; especially throughout these challenging times due to the pandemic.

I want to extend my sincere thanks to my co-supervisor Dr. M. J. A., who has taught me so much in the field of geology. Thank you, for the valuable experiences and knowledge you have provided me with; for giving me fantastic feedback and for always making the time. I want to express my gratitude to my co-supervisor E. G. Ballo, for supporting and helping me setting up the project and for guiding me through the first steps of the analysis.

Futhermore, I want to express my gratitude to Dr. C.C. Bakels, for all your specialized, in-depth guidance within the palynological studies. Thank you for all your time and enthusiasm and thank you for providing me with extremely valuable and interesting literature and anecdotes.

This project would not have been possible without the impressive high-resolution data set, provided by pollen specialist H. I. Høeg. Thank you, for giving me the opportunity to work with your impressive data and for taking the time to meet to

discuss the project and the results. I'm extremely grateful to everyone on the VIKINGS project who inspired me, helped me and supported me in the process. I would like to send a special thanks to Anneke for helping me with my pollen plots: thank you for introducing Rstudio to me to make my life easier. Last but not least I would like to thank Anna Lina, for all the motivational and emotional support. Thank you for spending your evenings and Saturdays at campus with me, for teaching me about streamlines, exchanging ideas on our theses and for buying me my favorite wrap at Bunnpris.

1. <https://www.mn.uio.no/geo/english/research/projects/vikings/>

1. Introduction

1.1 Past landscape utilization in Norway

The landscape in Norway has been impacted by human activities from the emergence of agriculture onwards. Traces of human activity have been documented in paleoenvironmental archives, such as peat or lake sequences. Paleoenvironmental archives are naturally occurring sources which preserve information about past environmental vegetation and the cultural landscape of the area (Bell and Blais 2021, 1; Overland and Hjelle 2009, 459). These archives can be used in order to extract pollen records. Pollen can be used as a proxy in order to reconstruct agricultural practices as well as the past vegetation (Bell and Blais 2021, 1; Lowe and Walker 2015, 194-6). A pollen record of a natural archive can reflect changes in the natural vegetation, as well as changes related to human activities according to time (Lowe and Walker 2015, 194-6).

Several studies located in Norway have been devoted to paleoenvironmental reconstructions using pollen analysis, often providing insights into the human impact on the natural vegetation reflected in the pollen assemblage (Bajard et al. unpublished; Bjune 2005; Hjelle et al. 2012; Larsen et al. 2006; Mehl and Hjelle 2015; Overland and Hjelle 2009; Prøsch-Danielsen 1993). An example of such a study is a palynological analysis conducted by Hjelle et al. (2012), in which archaeological and botanical data were combined to reveal spatial patterns about the human impact on the natural vegetation through time (Hjelle et al. 2012, 1368). In their study, they focused primarily on the transition from hunter-gathering to the emergence of farming activities in the Late Neolithic and Early Bronze Age.

Whereas most studies tend to focus on major transitions in the pollen record (Mehl and Hjelle 2015) and the emergence of farming (Hjelle et al. 2012), less attention has been given to transitions within later periods of farming, such as the Iron Age and the Middle Ages. A study by Prøsch-Danielsen (1993) attempted to make a distinction between different farming techniques used through time, thereby distinguishing cultivation from animal husbandry (Prøsch-Danielsen 1993, 233). However, similarly to Hjelle et al. (2012), Prøsch-Danielsen focused on older periods, analyzing the pollen record from the Mesolithic to the Late

Bronze Age (Prøsch-Danielsen 1993). In order to make distinctions between different farming techniques and to identify transitions occurring during periods of cultivation and grazing, a high-resolution pollen analysis is required. A recent paleoenvironmental study located in southeastern Norway was able to distinguish different types of agricultural practices from one another, utilizing a high-resolution pollen data set (Bajard et al. unpublished). This study provided a multi-proxy analysis of a lake sediment sequence from the Roman Iron Age to the Late Iron Age. As a result of the high-resolution of their pollen record, they were able to identify a pattern of periods dominated by cultivation of cereals and hemp, alternated by colder periods dominated by grazing activities. Since these alternations were synchronous with changes in temperature seen in the lake, the results could be interpreted as a human adaptation to climate variability in terms of agricultural strategies (Bajard et al. unpublished). The findings of this study raise the question whether a similar agricultural pattern as analyzed by Bajard et al. can be found in other paleoenvironmental archives in southeastern Norway.

Whereas several other palynological investigations took place in southeastern Norway in the past, very few of these sequences have been dated (Danielsen 1970, 8). Most palynological studies utilizing dated paleoenvironmental archives are located in central or at the west coast of Norway (Bjune 2005; Larsen et al. 2006; Mehl and Hjelle 2015; Overland and Hjelle 2009). Danielsen (1969) conducted several pollen analyses in Østfold, southeastern Norway, for which he relied on relative chronologies as opposed to absolute chronologies. In his studies he focused primarily on the reconstruction of the natural vegetation of Østfold county, and briefly on the Mesolithic hunter and fisher cultures and the Neolithic farmer culture (Danielsen 1970, 119). Considering the lack of radiocarbon dates in Danielsen's studies, it is challenging to use these pollen records in comparison to more recent dated paleoenvironmental archives. As a result, not much is known about the absolute chronology of agricultural practices in southeastern Norway during the Iron Age and the Middle Ages.

1.2 Research questions

In this thesis, a pollen dataset of high-resolution retrieved from a peat bog will be used as a proxy to reconstruct the paleoenvironment of the area of Haraldstadmyr in Southeastern Norway. An attempt will be made to reconstruct the human landscape utilization from the Iron Age to the Middle Ages. The goal is to find transitions within the pollen record from the Early Iron Age into the Medieval period in order to reconstruct the natural landscape as well as the agricultural dynamics of the area through time. Phases of arable farming, pastoral farming, mixed farming and abandonment will be distinguished and highlighted. Archaeological dates from a burial site named Bjørnstad, located next to Haraldstadmyr, will be studied in comparison to the pollen record in order to provide a multidisciplinary study of the cultural landscape use of the area, combining both disciplines of archaeology and palynology. Subsequently, plausible forcing factors of the transitions found within the pollen record will be discussed. An attempt will be made to link the transitions seen in the natural vegetation and cultural landscape to forcing factors such as climate change and societal changes, in order to give an insight on whether the transitions identified in the pollen record could be caused by human impact, climate change, or human adaptation to climate change. The thesis will attempt to answer the following research questions:

Which transitions can be found within the pollen record?

How has the local and regional vegetation of the peat bog developed through time?

How has the cultural landscape developed from the Early Iron Age to the Middle Ages?

Which variations in agricultural activities and farming intensity can be interpreted from the pollen record from the Early Iron Age to the Middle Ages?

How do the findings from the palynology compare to the dated burials at Bjørnstad burial site as well as other archaeological finds in the area?

Which forcing factors could potentially have caused the transitions seen in the pollen record?

1.3 Outline of the thesis

First an introduction will be given (chapter 1) on the area of interest and the environmental settings and background of the site. Subsequently, the use of pollen as a proxy will be discussed, as well as the types of pollen that can serve as anthropogenic indicators. Following, in chapter 2, the methods used in the thesis will be explained, discussing the retrieval and the subsequent handling of the pollen data in order to plot the pollen diagrams, as well as the handling of the archaeological data in order to plot the radiocarbon ages. The subsequent three chapters present the results of the study. In chapter 3, the results of the radiocarbon dating will be presented, and the age-depth model will be described. In chapter 4, the entire pollen record will be described, in order to gain an overview of the main changes in the natural vegetation as analyzed from the peat sequence. In chapter 5, a short overview will be provided of the dated archaeological finds as documented in previous studies. Additionally, calibrated radiocarbon dates from a burial site located nearby the site of interest will be presented and categorized into different time periods. In the discussion (chapter 6) the development of the local and regional vegetation will be discussed, where the pollen record will be interpreted in order to reconstruct the past natural vegetation. Subsequently, the evolution of farming from the Early Iron Age to the Medieval period will be analyzed, interpreting the pollen record utilizing anthropogenic indicators and combining the pollen data with the archaeological data from the area. Plausible forcing factors of the transitions recognized in the pollen record will be discussed, as well as a reflective subchapter on the reliability and the limitations of the current study. Finally, in chapter 7, a summary of the main findings will be presented, as well as possibilities for further research and further exploration of the findings.

1.4 Settings and background of the study

1.4.1 The study site

Haraldstadmyr bog (59°17'42.1"N 11°03'18.3"E) is located in the Østfold county of Norway (Figure 2-3), approximately 3 km west-northwest of Sarpsborg, at a height of 43 m.a.s.l. The bog covers a total area of approximately 41,244 m². The current vegetation of the peat bog includes peat moss (*Sphagnum*), grass (*Poaceae*), meadowsweet (*Filipendula ulmaria*), blue whortleberry (*Vaccinium cyanococcus*), bog blueberry (*Baccinium uliginosum*) and willow (*Salix*). The bog is surrounded by forest consisting primarily of the Norway spruce (*Picea abies*), birch (*Betula*), alder (*Alnus*) and some pine (*Pinus*) (Høeg unpublished) (Figure 3).

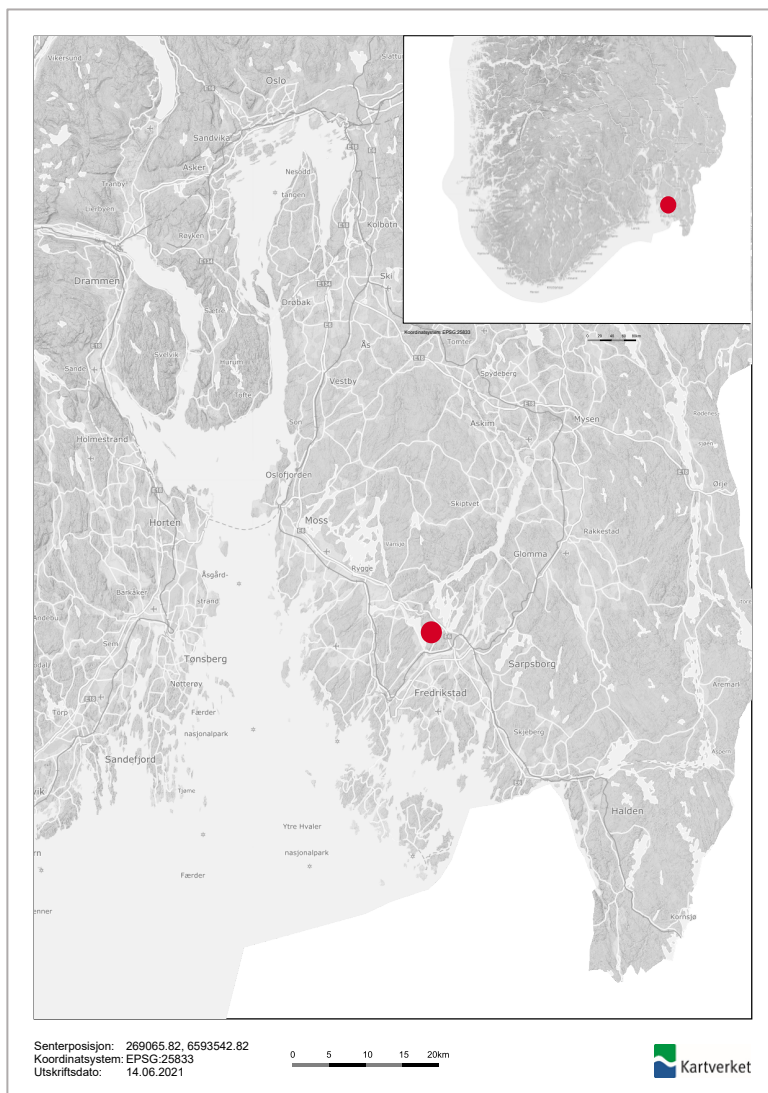


Figure 2: Map of Norway showing the location of the study site situated in Østfold, Southeastern Norway indicated by the red dot (kartverket.no).



Figure 3: An aerial photograph depicting the current vegetation of Haraldstadmyr Bog, Østfold, Southeastern Norway (kartverket.no).

Haraldstadmyr bog has been affected and disturbed by peat harvesting since 1882 (Danielsen 1970, 44). However, narrow strips of the original surface have been preserved in between the trenches where the peat was taken out. On these narrow strips, the formation of peat seems to have ceased as a result of drainage of the basin: the bog seems to be suffering from gradual degradation (Danielsen 1970, 44). In 1892, Blytt and Stangeland described a *Sphagnum* peat layer at Haraldstadmyr bog of 1.5-2m thickness. Subsequently, in 1949, Anders Danielsen (1949) reported a 1.6 m thick layer (Danielsen 1970, 44).

Several botanists have studied Haraldstadmyr in the past. Axel G. Blytt was the first one to study the bog, after which in 1949 Danielsen retrieved a core for pollen analysis on one of the narrow strips containing the original surface of the bog, in the same area as the current study is located (Danielsen 1970, 44).

Danielsen described an observation of elm fall (*Ulmus*) which he associated with the emergence of agriculture (Danielsen 1970, 119). In four of his diagrams, all located in Østfold county within a radius of 25 km from one another, he described a contemporary decline in *Ulmus* with the first appearance of cultivation pollen.

Considering the lack of radiocarbon dates in his study, he relied on relative chronologies to estimate the emergence of agriculture to occur in the Neolithic (Danielsen 1970, 119). Later, H. I. Høeg and E. Østmo conducted supplementary pollen surveys to confirm this finding. As a result, the decline in *Ulmus* was dated to 5010 ± 100 BP, translating to circa 3050 cal. BCE, thereby confirming Danielsen's hypothesis (Østmo 1988, 235).

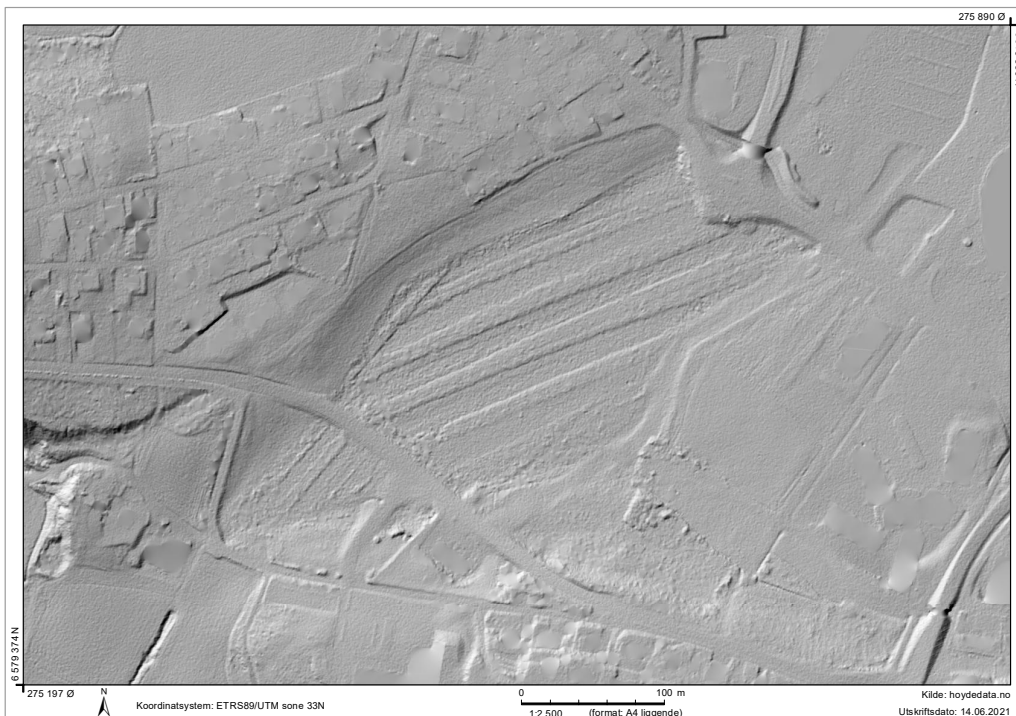


Figure 4: Elevation map depicting Haraldstadmyr bog, Østfold, Southeastern Norway (hoydedata.no).

Haraldstadmyr bog is recognized as a cultural heritage site. Previous archaeological finds have indicated that the bog might have been used as a sacrificial site (Iversen 2018, 1). Utilizing bogs as sacrificial sites is a fairly common archaeological phenomenon in northern-Europe. Often many spectacular artifacts are found in bogs or wetlands. In 2006, a flint dagger was found in Haraldstadmyr bog, which was dated to the Neolithic (Iversen 2018, 1). Additionally, a belt buckle with a piece of preserved leather was found, which was believed to be from the later Iron Age (Iversen 2018, 1). More recently, the bog has been disturbed for the construction of a building (Figure 5) (Iversen 2018, 1). These construction works were against the Norwegian law, as Haraldstadmyr is registered as a cultural heritage site. Unfortunately, due to extensive drainage the bog is expected to dry out, which will result in poor preservation of archaeological material and botanical data. Therefore, in 2020, an excavation took

place at Haraldstadmyr bog (Figure 6), in order to secure important historical information before the bogs dries out entirely (Iversen 2018, 3).



Figure 5: Location of the excavation site at Haraldstadmyr bog. The excavated area is depicted in green (Iversen 2018).



Figure 6: Haraldstadmyr excavation, November 2020.

1.4.2 Geology of the area

Haraldstadmyr is positioned on the Ra-ridge or the ‘inner-Ra’: a marine terminal moraine (Figure 7). This moraine was formed during the end of the last glacial period and has been dated to 11,000-10,700 years BP (Younger Dryas) (Brandal & Heder 1991, 3). Most of the ridge was deposited below sea level. The ridge can be found on both sides of the Oslo fjord (Danielsen 1970, 13). On the eastern side it runs through the Østfold county from the Swedish border through Sarpsborg to Moss. The average height of Østfold county is around 122 m. a. s. l (Danielsen 1970, 10). A difference in landscape can be seen north of the Ra as opposed to south of the Ra. North of the Ra the landscape is characterized by shallow soils, lakes and tarns. South of the Ra, fewer tarns can be found, and almost no lakes occur (Danielsen 1970, 12). This difference in landscape was caused by glacial erosion taking place north of the Ra, as opposed glacial accumulation and slope deposits during sea regression occurring south of the Ra. Additionally, marine clay was deposited south of the Ra during the Late-glacial and Post-glacial (Danielsen 1970, 10-13).

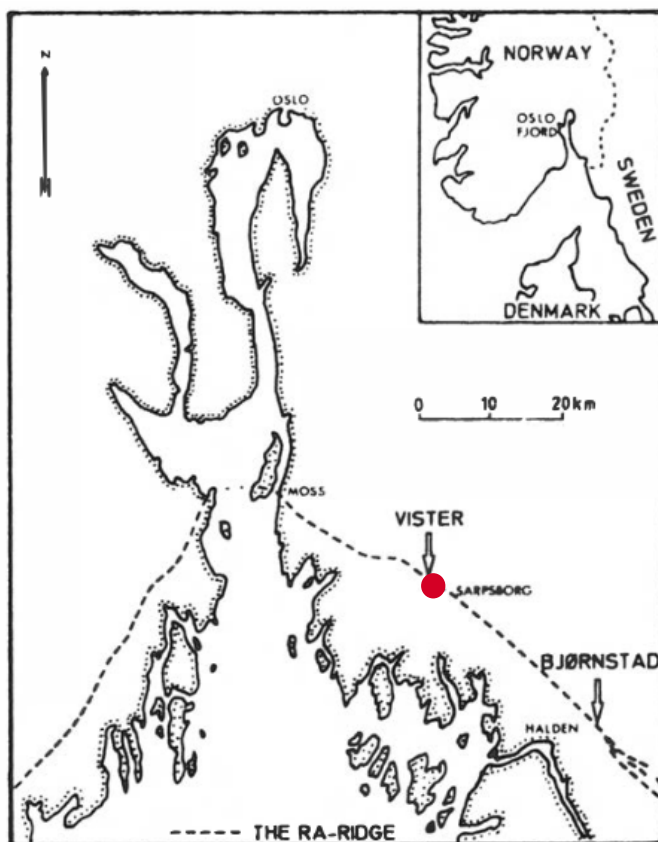


Figure 7: The Ra-ridge running through both Østfold and Vestfold county, with the red dot indicating the location of Haraldstadmyr bog (Brandal & Heder 1991, 3).

Most of the bedrock in Østfold consists of Precambrian gneisses and granites (Brandal & Heder, 1991, 4). As a result of the deposition of abundant amounts of loose material in Østfold county, transported by land ice from north to south, Østfold county contains favourable substrata for a variety of vegetation types. In combination with the accumulation of marine clays, these substrata make the Ra district a fertile area with arable soils, suitable for agricultural purposes (Danielsen 1970, 15). Other loose material that is still transported to Østfold today includes flint, which was transported by sea ice following the Baltic current. This transportation most likely occurred during the entire post-glacial (Danielsen 1970, 15). During the Late Quaternary both minerogenic and organogenic processes contributed to the soil formation in southern Østfold. The marine clay deposits are an example of a minerogenic process, which later resulted in dry and fertile land during sea regression (Danielsen 1970, 15). An example of an organogenic process is the formation of humus soils, which is usually formed by the activity of coniferous forests or other acidiphilous vegetation. Additionally, different types of peat were formed as a result of organogenic processes, such as terrestrial peat, telmatic peat and limnic peat. Other deposits include gyttja or nekronmud, which are mainly deposited on the bottom of eutrophic or oligotrophic stagnant waters, dry or gel-mud which is usually deposited in dystrophic tarns and marine shell marl, which mostly accumulates in thick shell banks (Danielsen 1970, 13-15).

1.4.3 Vegetation of the area

Through time, the landscape in Norway changed from an open landscape in the Late Glacial to an immigration of trees and a forested landscape in later periods (Mehl and Hjelle 2015, 45). The first publication on vegetation types found in the Østfold district was published in 1779 (Wilse 1779 in Danielsen 1970, 20). In his paper, Wilse described the occurrence of cultivated plant types *Fagopyrum*, *Linum* and *Cannabis* in the district of Spydeberg (Danielsen 1970, 20). Subsequently, Breien (1933) studied the vegetation on shell banks located in inner Østfold (Breien 1933 in Danielsen 1970, 20). In this area marine deposits were deposited. Later on, these became dry land due to sea regression, creating substrata suitable for a greater variation of vegetation than the oligotrophic environments. Examples of plant types recorded there are *Anemone hepatica*, *Brachypodium pinnatum*, *Epipactis atrorubens*, *Inula salicina*, *Polygala*

amarella, *Silene nutans* (Danielsen 1970, 20). In 1959 Landskognakseringen published statistical tables reporting on the vegetation of the entire Østfold district (Danielsen 1970, 20). They reported a percentage of 55% productive forest, 4% peat land, 7% barren land and 34% of other surface such as water, cultivated soils and human impacted landscape. According to their statistics, the forest consisted out of 31% *Picea abies*, 25 % *Pinus silvestris*, 27% mixed coniferous forest, 16 % other types of mixed forest of coniferous and deciduous trees and 1% pure deciduous forest.

A more recent paper by Fjellstad and Dramstad (1999) analyzed aerial photographs in order to reconstruct the vegetation of Rakkestad area during the second half of the 20th century (Fjellstad and Dramstad 1999). Rakkestad is an inland area in Østfold county, located approximately 20 kilometers northeast of Haraldstadmyr bog. As a result, they found 57.9 % of the landscape to be intensively cultivated land, as well as a total of 28.8 % of coniferous trees (Table 1) (Fjellstad and Dramstad 1999).

Table 1: Distribution of vegetation types accounted for in Rakkestad and Hjartdal municipalities during the 1950s and 1990s (Fjellstad and Dramstad 1999).

Land cover	Rakkestad			Hjartdal		
	1953	1992	Change ^b	1955	1993	Change ^b
Coniferous trees	26.3	28.8	+2.4	22.5	26.6	+4.1
Deciduous trees	1.1	0.7	-0.4	6.5	12.7	+6.3
Mixed woodland	1.6	0.1	-1.5	14.8	15.5	+0.7
Scattered conifers	0.1	1.4	+1.2	1.3	1.6	+0.3
Scattered deciduous trees	0.0	0.0	0.0	3.4	1.6	-1.8
Scattered mixed trees	0.0	0.0	0.0	5.6	2.7	-2.9
Intensively cultivated land	50.9	57.9	+7.1	4.4	4.3	-0.1
Grassland	5.1	2.2	-2.9	24.7	19.7	-5.0
Pasture	6.8	0.8	-6.0	10.8	8.2	-2.6
Rivers and streams	1.8	1.4	-0.4	0.8	0.8	0.0
Road	1.7	0.9	-0.9	1.1	1.6	+0.5
Track	0.4	0.1	-0.3	0.4	0.3	-0.1
Stone wall	0.0	0.0	0.0	1.2	0.8	-0.4
Garden/farmyard	1.7	3.3	+1.6	0.5	2.5	+2.0
Building	0.5	0.5	0.0	0.7	0.7	0.0
Rocky outcrop	1.1	1.9	+0.8	0.6	0.0	-0.6
Mire	0.7	0.1	-0.6	0.0	0.0	0.0
Pond	0.2	0.1	-0.1	0.0	0.0	0.0
Scree	0.0	0.0	0.0	0.6	0.2	-0.4

^a Figures in bold indicate that the changes in Rakkestad and Hjartdal are significantly different (z-test, $\alpha = 0.05$).

^b Changes are indicated as percent change in overall frequency.

1.4.4 Farming in the area

Agriculture is known to have emerged in southern Norway during the 4th millennium BCE. Prior to that, during the Mesolithic and the beginning of the Neolithic, the economy was primarily based on hunting and fishing (Mehl and Hjelle 2015, 45). During this time, most of the settlements in Norway were located along the coast, as fishing was an important source of food (Mehl and Hjelle 2015, 45). The impact of agriculture on vegetation and landscape can mostly be recognized in pollen records from the Middle Neolithic onwards, around 2400 cal. BCE, when forests seem to be opened up and cultivated fields, pastures, meadows and heathlands start to develop (Hjelle et al. 2012, 1369). In some local diagrams analyzed from bogs, located close to archaeological settlements, the human impact on the vegetation can already be recognized in the Late Mesolithic (Mehl and Hjelle 2015, 45). Once the land started to be used for agricultural purposes, such as animal husbandry and cultivation, a clear transition in pollen records could be seen (Mehl and Hjelle 2015, 45). In the district of Østfold, traces of agricultural practices appear much earlier in the Stone Age and in larger amounts than found elsewhere in Norway (Østmo 1988, 11). In this area, traces of agriculture were found from around 3050 cal. BCE (Østmo 1988, 234).

In both Vestfold and Østfold district, prehistoric roads used to follow the ridges of the Raet (Danielsen 1970, 15; Solheim and Iversen 2019, 427). Along the sides of the moraine, fertile and easily arable soils could be found (Danielsen 1969, 15). As a result, medieval and Iron-Age farms settlements were typically located along the Ra moraines (Danielsen 1970, 15; Solheim and Iversen 2019, 427). The age of the moraine has been derived from radiocarbon dates retrieved from cemeteries located alongside the old Raet road (Solheim and Iversen 2019, 429). It seems that the road has been in use from prehistoric times into the Medieval period. From 2000 BCE onwards a steady increase in radiocarbon dates was seen, indicating an increase in human population and activity (Solheim and Iversen 2019, 429). Up to this day, the E6 highway still follows the Ra moraine from Halden to Moss, thereby crossing through Haraldstadmyr bog.

A large number of archaeological burial finds have shown that this area has been extensively used for farming (Iversen 2018, 1). Several excavations took place

located along the Raet, during which numerous grave finds were found, showing a clear farming environment in the area since the beginning of agriculture (Iversen 2018, 1).

The surrounding area of Haraldstadmyr is known to be one of the richest cultural heritage areas in Norway, especially around Grålum and Tune. In the nearby area a large number of graves and settlement traces have been found, which were dated to the Stone Age, Bronze Age and Iron Age. Three large farms used to surround Haraldstadmyr, named Bjørnstad, Opstad and Tune. Following the Raet from Sarpsborg to Opstad several graveyards can be found: “Trompeten” below Store Tuene, Tingvoll, Grålum, Bjørnstad, Kalnes and Opstad (Iversen 2017, 2-4).

1.4.5 Bjørnstad burial site

The Bjørnstad farm is located next to Haraldstadmyr. The farm seems to have consisted out of two parts up to 1390-1400 CE, divided up into a northern and a southern part (Iversen 2017, 2-4). A burial site was found on the boundary between the northern and the southern part of the farm. Additionally, two other cemeteries are known to be located at the Bjørnstad farm, one located in the southern part and one located in the northern part. The different cemeteries are situated quite close to each other, indicating that there might have been one large farm cemetery (Iversen 2017, 2-4). The burial site is expected to represent the population of the local farmers living in the nearby farms through time. The northern part of the cemetery has been excavated between 2000 and 2006, during which 11 graves and 9 ring ditches were found (Iversen 2017, 2-4). In 2017, another excavation took place at the northern part of the cemetery. During this excavation 19 carbon samples from the excavation were dated, as well as 24 bone samples, in order to retrieve a better resolution on the chronology of the cemetery (Iversen 2017).

1.5 The formation of peat bogs

Peat bogs are often formed over a long period of time. They often start as open waters, and gradually develop into mires, fens or bogs. This development is known as ‘a ‘hydrosere’, a process during which sediments gradually change from mud to peats (Lowe and Walker 2015, 154). The hydroseral succession involves

several steps. Limnic peats usually form beneath the regional water table in lakes. They consist of transported plant debris and decayed vegetation growing *in situ*. Subsequently, they turn into telmatic peats, forming in the swamp zone between low and highwater levels. Finally, terrestrial peats accumulate above the water table (Figure 8) (Lowe and Walker 2015, 154).

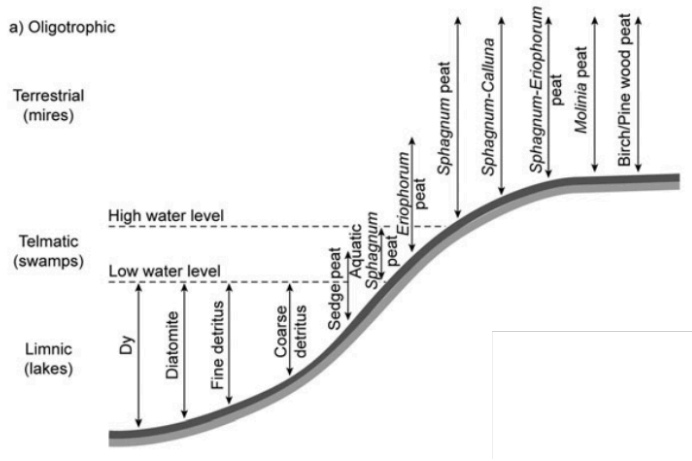


Figure 8: A schematic depiction of the hydrosereal succession and the development from limnic peats in lakes to terrestrial peats under oligotrophic conditions (Lowe and Walker 2015, 154).

Thus, bogs often start as small lakes, after which they develop into topogenous mires, also referred to as fens (Figure 9). Here, water accumulates in enclosed basins, inducing peat formation (Lowe and Walker 2015, 154). Over time, these turn into ombrogenous mires, or in other words bogs, in which the water table is maintained by high atmospheric moisture levels (Neef and Cappers 2012, 147; Lowe and Walker 2015, 154). Subsequently, the accumulation of peat can result in a lifted or raised surface above the level of the surrounding area: a raised bog, announcing the final stage of topogenous hydrosere. Raised bogs occur mostly in lowland areas, where *Sphagnum* mosses, a peat-forming plant, dominate (Lowe and Walker 2015, 154). When raised bogs are primarily formed by *Sphagnum*, they are commonly referred to as sphagnum bogs or sphagnum peat (Neef and Cappers 2012, 147). Vegetation characteristic of sphagnum bogs are the heather types *Ericales*, *Calluna* and *Myrica*, as well as Cottongrasses (*Eriophorum*) (Neef and Cappers 2012, 147). Due to the humid and acidic environment of peat bogs, the dead parts of moss plants as well as higher plants do not tend to decay. As a result, a continuous accumulation of organic material takes place (Neef and Cappers 2012, 147). On average, the accumulation rate of organic material in peat bogs is estimated to be 1 mm per year, which means that an undisturbed bog can

accumulate up to 10 cm every century. In sphagnum peat, a constancy of growth and die-back of Sphagnum can be assumed (Neef and Cappers 2012, 148).

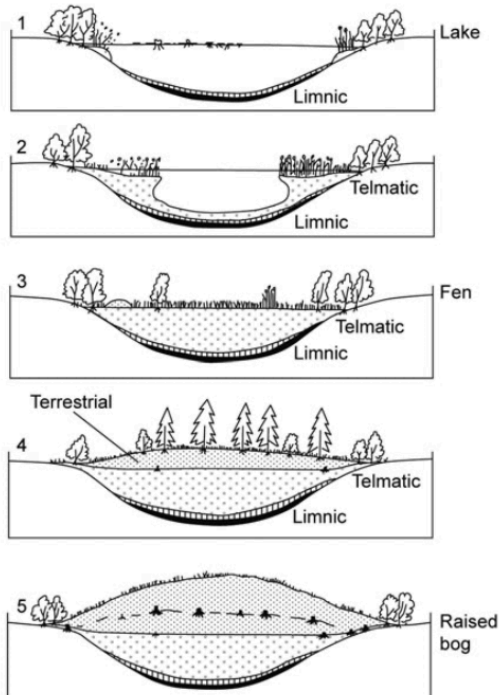


Figure 9: Schematic representation of the development of a lake to a raised bog (Lowe and Walker 2015, 154).

Changes in the lithology of peat sequences can often be inferred with changes in the local vegetation (Lowe and Walker 2015, 155), as well as changes in climatic conditions and precipitation levels.

1.6 Pollen as a proxy

The pollen record from a peat sequence can serve as a proxy for the reconstruction of paleoenvironments. Since 1920 this technique, also referred to as palynology, has been used to reconstruct late Quaternary vegetation change on a local as well as regional scale (Lowe and Walker 2015, 183). Additionally, it can be used in order to reconstruct human activities and their impact on the past landscape and vegetation. Different types of pollen represent different types of changes. Plant types growing in or near the peat bog, such as aquatic plants and waterside plants, tend to represent changes in the local vegetation. Other pollen types, such as pollen of trees, shrubs, grasses and herbs tend to represent the regional vegetation of the area (Lowe and Walker 2015, 173). When interpreting a pollen record, important factors to be taken into consideration are the production rate of the pollen and the dispersal rate of the pollen. Each plant type differs to a great extent in terms of the amount of pollen it produces, and the ways in which these pollen are dispersed (Lowe and Walker 2015, 169).

1.7 Anthropogenic indicators

Human impact on the landscape can be represented in the pollen record by several indicators. First of all, a decrease in arboreal pollen percentages can indicate a significant alternation of woodlands through potential burning or clearance (Lowe and Walker 2015, 175). Subsequently, a contemporary increase in pollen from cereals and high amounts of macroscopic charcoal fragments can indicate slash and burn practices (Gaillard 2013, 889). Slash and burn practices refer to a form of woodland use where trees are felled, dried and burned in order to clear forested areas. These soils are then enriched with ash from the burned organic matter in order to enhance the land for agricultural purposes (Gaillard 2013, 889). In juxtaposition, an increase in arboreal pollen can indicate fallow land being reverted to woodland (Behre 1981, 228). However, it remains challenging to distinguish human impact on the landscape from effects of climate change on the landscape (Gaillard 2013, 880).

Apart from fluctuations in arboreal pollen percentages and the number of charcoal fragments, there are many different pollen species that may indicate human activity (Behre 1981, 226). These pollen types are referred to as anthropogenic

indicators (Behre 1981, 226). Episodes of pastoral or cereal cultivation are often recognized in pollen assemblages by the presence of pollen of ruderal taxa to indicate pastoral farming and cereal taxa to indicate phases of cultivation (Lowe and Walker 2015, 175). Pollen of cultivated crops are good indicators of early cultivation. Amongst these are the cereals *Triticum* (common wheat), *Hordeum* (barley), *Avena* (oats) and *Secale* (rye). (Behre 1981, 226). Other crops that can be indicators of cultivation are *Centaurea cyanus* (cornflower), *Cannabis* (hemp), *Polygonum convolvulus* (black bindweed) and *Trifolium* (clover) (Behre 1981, 233-7). However, during pollen analysis it can be hard to distinguish *Cannabis* from *Humulus* (Behre 1981, 227).

Pollen of ruderal taxa are important indicators of pastoral farming in pollen assemblages. Amongst these are herbs such as *Plantago lanceolata*, *Plantago major*, *Rumex*, *Rumex longifolius*, *Artemisia*, *Chenopodiaceae*, *Urtica* and *Juniperus* (Behre 1981, 233-5). *Plantago lanceolata* is known as a pure indicator of pastureland. Its abundance is often used as a measurement for the extent of cattle breeding (Behre 1981, 234). However, it is important to note that this herb will not grow in grazed forest, due to the fact that it has high light requirements. *Rumex* species can be regarded both as an indicator of pastoral farming as an indicator of arable activity (Behre 1981, 236). In this study, it was interpreted as an indicator of pastoral farming. *Plantago major*, *Artemisia*, *Chenopodiaceae* and *Urtica* can primarily be described as nitrophile species (Behre 1981, 236). Therefore, they are associated with nitrogen-rich areas and habitations. All of these pollen types tend to increase with grazing pressure and are therefore regarded as indicators for grassland degradation (Li et al. 2008, 1284). Furthermore, spores such as *Polypodium* and *Pteridium*, as well as *Sordaria* can be closely related to the development of grazing activities (van Geel 2003, 875). The fungi *Sordaria* can indicate the former presence of animals, due to the ascospores of *Sordaria* that tend to develop on the feces of herbivores. This way, *Sordaria* can serve as an indicator for grazing activities (van Geel, 2003, 875). The presence of spores of *Pteridium* and *Polypodium* often indicate land disturbed by fire and grazing, as well as dry heat, pastures and fallow land (Behre 1981, 233).

1.8 Production, dispersal, deposition and preservation of pollen

The production, dispersal, deposition and preservation of pollen form important factors when it comes to the interpretation of a pollen diagram. Each of these factors need to be taken into careful consideration when drawing conclusions about the paleoenvironment and cultural landscape of an area (Lowe and Walker 2015, 169).

First of all, each type of plants produces a different quantity of pollen. Usually, anemophilous plants produce more pollen than entomophilous species, resulting in an over-representation of anemophilous plants in the pollen record. In addition to that, autogamous plants are self-pollinating and thus liberate very few pollen grains into the atmosphere. An example of such a plant is *Triticum*.

Cleistogamous plants release even fewer pollen into the atmosphere, since their flowers never open. However, these are not given facts, as there is still variation among both autogamous and cleistogamous plants. Some plants still produce large quantities of pollen, even if they are insect-pollinated, such as *Tilia cordata* and *Calluna vulgaris*. In juxtaposition, the tree species *Fagus sylvatica* and *Quercus petraea*, are wind-pollinated plants that produce relatively little amounts of pollen. In Table 2, a schematic representation can be seen of the differences found in pollen production amongst the most common taxa in Europe.

Table 2: Table showing an estimate of pollen production amongst common plant species in Europe (Lowe and Walker 2015, 191).

Species	Number of pollen grains per anther	Number of pollen grains per flower	Number of pollen grains per catkin	Index of relative pollen production (cf. <i>Fagus</i> = 1.0)
<i>Trifolium pratense</i>	220			
<i>Acer platanoides</i>	1,000	8,000		
<i>Malus sylvestris</i>	1,400–6,250			
<i>Calluna vulgaris</i>	2,000 tetrads			
<i>Fraxinus excelsior</i>	12,500			
<i>Secale cereale</i>	19,000	57,000		
<i>Rumex acetosa</i>	30,000	180,000		
<i>Juniperus communis</i>		400,000		
<i>Pinus sylvestris</i>		160,000		15.8
<i>Picea abies</i>		600,000		13.4
<i>Betula pubescens</i>			6,000,000	
<i>Alnus glutinosa</i>			4,500,000	17.7
<i>Quercus robur</i>		1,250,000		
<i>Fagus sylvatica</i>				1.0
<i>Quercus petraea</i>				1.6
<i>Carpinus betulus</i>				7.7
<i>Betula pendula</i>				13.6
<i>Corylus avellana</i>				13.7
<i>Tilia cordata</i>				13.7

A second important factor is the dispersal of pollen grains. It is important to consider the different types of pollen dispersal: self-pollinated, wind-pollinated and insect-pollinated. Factors within these three types of dispersal can impact the distance between the source of the pollen to its point of deposition. An example is the wind speed for wind-pollinated plants, as well as the surface area of a site in relation to its surrounding vegetation cover. Another important means of dispersal is the transport of pollen grains by streams. Many studies have been devoted to modern pollen dispersal in order to document the uncertainties in pollen analysis of past environments (Bradshaw 1981; Heide and Bradshaw 1982 in Lowe and Walker 2015, 171). Findings have shown that wind-pollinated pollen are usually deposited within a few kilometers from their source. The chances that the pollen grains are liberated into the atmosphere and travel farther are very small. Nonetheless, a few rare cases of far-travelled pollen have been found.

The last factor that is important to take into consideration when interpreting pollen records is the nature of pollen deposition. Most uncertainties occur when studying a lake sequence, due to differential settling velocities combined with disturbance of sediment on the bottom of the lake, by for example currents or burrowing organisms (Lowe and Walker 2015, 171). In a bog, however, fewer uncertainties occur. Nonetheless, there is a chance of lateral and vertical mixing for pollen deposition in bogs, where the larger grains tend to remain on the surface, while smaller can migrate downwards into the peat (Lowe and Walker 2015, 172). Fortunately, these movements and thus uncertainties are often very insignificant compared to the timescales in peat accumulation. Other uncertainties that can occur in a peat sequence are caused by mixing due to earthworms and other soil organisms. Thus, it is important to check peat sequences for any signs of burrows.

Finally, there is a risk is the deterioration of pollen grains in peat bogs due to physical, chemical and biological attack on the exine (Lowe and Walker 2015, 172). Delicate grains from for example *Urtica* and *Populus* can be destroyed entirely due to oxidation and corrosion (Havinga 1985 in Lowe and Walker, 172). Certain types of pollen, however, show more resistance to deterioration, such as certain ferns (*Polypodium*). As a result, some pollen types can be over-represented

in the pollen diagram, while others may be under-represented (Lowe and Walker 2015, 172).

When deriving an interpretation of the cultural landscape from a pollen diagram, all of these factors need to be taken into account. Amongst the pollen from cereal plants, *Secale* might be one of the best indicators of cultivation due to its high pollen productivity and good dispersal capacity (Behre 1981, 227). However, it is important to keep in mind that *Secale* was introduced in Europe in a much later period. *Triticum*, *Hordeum* and *Avena* occur earlier in the pollen record, but are unfortunately poorly dispersed. Therefore, it can occur that these indicators remain absent in peat profiles, even though there was cultivation in the area (Behre 1981, 227).

2. Methods

2.1 Introduction

For this study, a peat sequence retrieved from Haraldstadmyr bog was used. In order to place the study in geological context, a stratigraphy of the site was established by describing and interpreting the lithology of the peat archive. Subsequently, a chronology was established by dating the peat sequence and interpolating the dated layers using an age-depth model. Pollen data retrieved from the peat sequence by H. I. Høeg (unpublished) was used in order to obtain paleoenvironmental information about the sequence. The proxy record was analyzed in order to form an idea of the local as well as the regional vegetation and environmental changes of the area. The changes seen in the composition of the vegetation were interpreted, as they can reflect both anthropogenic processes as well as natural processes, perhaps induced by the climate. Furthermore, archaeological dated material from a nearby site was calibrated and studied in comparison with the pollen data obtained from the peat sequence. An attempt was made to correlate the results from the pollen record to the dated archaeological finds in the area in order to create an overview of the human impact on the vegetation of the region (Lowe and Walker 2015, 2). This chapter will provide a detailed description of these different methodologies used during this study.

2.2 Sampling

The peat sequence was retrieved from the deepest part of Haraldstadmyr bog by H. I. Høeg and Prof. Dr. Iversen in May 2018 (Figure 10-11). Several trial corings were performed beforehand in order to find the deepest part of the peat bog. It was important to locate the deepest part of the bog, in order to be able to sample a complete peat sequence representing a pollen assemblage as far back in time as possible. The core was sampled with a 'Russian' peat corer, a coring device that is extensively used in terrestrial studies in peat bog (Frew 2014, 4). This coring device consists of half a cylinder-shaped barrel, in which samples are collected by rotating the corer 180° clockwise. In total 4 core sections were sampled downward, reaching a total depth from 0 to 282 cm. The four different sections of the core were photographed in the lab. Subsequently, I logged and described the lithology of the core from bottom to top. In addition to that, an excavation at

Haraldstadmyr bog took place in 2020, during which I described the peat profile of one of the trial pits in order to compare it to the lithology of the peat core from 2018.



Figure 10: H.I. Høeg sampling the peat sequence at Haraldstadmyr bog, Southeastern Norway (Iversen 2018).

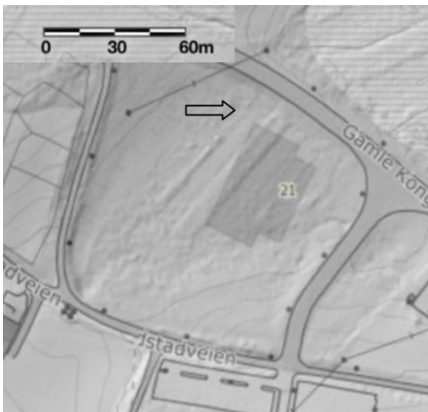


Figure 11: The sampling location of the peat sequence at Haraldstadmyr bog, Southeastern Norway (Iversen 2018).

2.3 Chronology

In order to establish a chronology of the peat sequence, radiocarbon ages were used, which were sampled by H. I. Høeg in 2018 and dated by *Lund University Radiocarbon Dating Laboratory*, Sweden. As a part of this thesis, the radiocarbon ages were calibrated using the IntCal20 calibration curve (Reimer et al. 2020). Once the radiocarbon dates were calibrated to calendar years, an age-depth model was generated using R software and the R code package ‘Bacon’ 2.4.3 (Blaauw and Christen 2011), interpolating the different dated layers. ‘Bacon’ is a software that utilizes Bayesian-based modelling. Bayesian-based modelling can be described as a statistical method that incorporates the principle of superposition: the model assumes material deeper down in the core to be older than material further up (Lowe and Walker 2015, 270). In general, an assumption of linearity

can be made for peat sediments. Especially in Sphagnum peat, a constancy of growth results in an accurate estimate of the time span between two levels (Neef and Cappens 2012, 148)

2.4 Pollen analysis

In total, 82 samples were prepared and analyzed by H. I. Høeg in 2018 (unpublished). For each pollen sample, approximately 1 cm³ of peat was taken out from the core. From 0-80 cm, samples were taken out for every 10 or 5 cm. Subsequently, from 80-130 cm samples were taken for every cm, in order to obtain a higher resolution for the period of interest for the VIKINGS project: 500-1250 CE. According to Høeg's age model (unpublished), based on the IntCal13 calibration curve, these depths correlated with ages of approximately 400-1000 CE. From 220-280 cm samples were taken out for each 20 cm. 2 tablets of *Lycopodium* were added to each sample. They contained 10679 ± 192 or 12500 ± 374 spores of *Lycopodium clavatum* (common club moss). Thus, in total, 21358 ± 136 or 25000 ± 264 spores were added to each sample. Subsequently, 105 different types of pollen were counted and documented for each sample in the microscope.

2.5 Pollen diagrams

2.5.1 The input data

2.5.1.1 *Selecting the pollen sum: dryland and wetland pollen*

The counted number of pollen for each sample needed to be converted to percentages using the pollen sum (ΣP). The pollen sum represents the total number of pollen counted in each sample. In order to prevent overrepresentation of pollen produced by plants that were located near the place of coring, any local pollen types were excluded from the sum (Bakels 2020, 209). Even for wind-pollinated species, the majority of pollen tends to land close to the parent plant. Thus, it is important to distinguish the local pollen types from the regional pollen types (Neef and Cappens 2012, 153). As Haraldstadmyr is a peat bog, and thus a wetland, an important distinction was made between dryland and wetland pollen. The pollen sum is based on the dryland pollen and can thus be called the dryland pollen sum. The dryland pollen include all pollen types that grow on dry

locations, such as trees, shrubs and herbs, and are meant to represent the regional vegetation of the area. Together, they form a total of 100%. The wetland pollen include all aquatic pollen types, as well as plant types growing along the waterside and local pollen types from the nearby area. These were excluded from the pollen sum. As a consequence, the local vegetation heather types *Ericales*, *Empetrum* and *Calluna* were excluded from the sum (Stivrins et al. 2017, 2), as well as wetland plants often found in bogs or damp locations such as *Carex*, *Eriophorum* and *Scirpus*. Other types that were excluded from the sum were *Filipendula*, *Apiaceae* and *Galium*. The aquatic plants that were excluded from the dry pollen sum include *Lysimachia*, *Typha latifolia*, *Potamogeton*, *Menyanthes*, *Myriophyllum alterniflorum*, *Drosera*, *Lythrum*, *Rubus chamaemorus*. In addition, the spores *Equisetum*, *Sphagnum*, *Lycopodium annotinum*, *Huperzia selago*, *Dryopteris*, *Gymnocarpium* and the microorganisms *Botryococcus*, *Pediastrum*, *Helotium*, *Assulina*, *Amphitrema* and *Sordaria* were excluded from the pollen sum. The spore plants *Polypodium* and *Pteridium*, however, were included in the pollen sum, since ferns are not part of the local vegetation of a raised bog.

2.5.1.2 Calculating the percentages and concentrations

The pollen sum was used in order to calculate the percentages of pollen that were counted by using the formula:

$$P\% = \frac{X}{\Sigma P} \times 100$$

, where X represents the number of pollen for a certain pollen type for each sample. These percentages aim to represent the regional vegetation.

The percentages of the local and aquatic pollen types, as well as most of the spore plants and the number of charcoals were calculated based on $\Sigma P + X$ (Danielsen 1970; Danielsen 1993; Hjelle et al. 2012; Overland and Hjelle 2009), where X represents the pollen type, spore or charcoal in question. For this calculation, the following formula was used:

$$P\% = \frac{\Sigma P + X}{\Sigma P} \times 100$$

Subsequently, several pollen types with percentages of less than 1% were multiplied by 10 or 20, in order to make them more visible in the percentage

diagrams. These numbers were sorted utilizing the conditional formatting function in Excel.

2.5.1.3 *Arboreal and non-arboreal pollen*

After calculating the pollen sum and the percentages for each pollen type per sample, a distinction was made between arboreal pollen and non-arboreal pollen in order to create a curve showing the ratio between tree pollen (arboreal pollen) and pollen from herbaceous plants (non-arboreal pollen). Both arboreal pollen and non-arboreal pollen represent the regional vegetation and are thus part of the dry pollen sum. Together, the sum of arboreal pollen and the sum of non-arboreal pollen add up to the total pollen sum: $\Sigma P = \Sigma AP + \Sigma NAP = 100\%$.

2.5.1.4 *Anthropogenic indicators*

For the reconstruction of human impact on the landscape, several pollen types were selected in order to make a more specified pollen diagram. For this diagram, the types of pollen were selected that could possibly indicate human impact on the vegetation and the landscape (Behre 1981). The tree types that were selected include *Betula*, *Pinus*, *Corylus*, *Alnus*, *Picea*, *Fagus*, *Quercus*, *Fraxinus* and *Juniperus*. Additionally, several herbs were selected that can act as anthropogenic indicators. Amongst these were the cereals *Hordeum*, *Triticum*, *Avena* and *Secale*, as well as other herbs such as *Centaurea cyanus*, *Cannabis*, *Polygonum*, *Plantago major*, *Plantago lanceolata*, *Rumex*, *Rumex longifolius*, *Artemisia*, *Chenopodiaceae*, *Urtica*, *Filipendula* and *Trifolium*. Furthermore, the spores *Polypodium*, *Pteridium* and the fungi *Sordaria* were included as well.

2.5.2 Construction of the pollen diagrams in R-rioja

The pollen diagrams were plotted against age using R version 4.0.3 (2020-10-10) with the package ‘rioja’ version 0.9-26 (Juggins 2020) in combination with packages ‘ggplot2’ version 3.3.3 (Wickham 2016) ‘tidyverse’ version 1.3.0 (Wickham et al. 2019) and ‘neotoma’ version 1.7.4 (Goring et al. 2015). A csv-file containing the raw percentage pollen data was read in R, after which the data was filtered, sorted and subsequently plotted utilizing code (code in appendix D).

In the csv-file the depths were replaced with their according mean ages as generated by the age-depth model.

2.5.2.1 Main diagrams

In order to show all of the pollen types for each sample through time, three diagrams were made. The pollen types for each sample were plotted against age, ranging from 3350 BCE to 1950 CE, which correlates to depths of the entire core: 282-0 cm. For the y-axis, an interval of 50 years was used. The x-axis was scaled according to the percentage data of each pollen type. The data was divided into three different diagrams in order to avoid the occurrence of too many variables. An exaggeration of x20 was applied to make the smaller curves more visible. For each cluster of taxa different colours were assigned in the plot. However, all herbs are shown in brown red. Afterwards, the figures were edited in Adobe Illustrator, where the depth markers as well as the clusters of taxa and the different zones were added manually. The diagram was divided into zones based on changes in the pollen record as well as the content of the pollen record. This way, the zones helped to mark transitions in the pollen record, as well as to distinguish sections in the pollen record which differed in content. Subsequently, the zones were used in order to describe the transitions in the pollen record. More zones were created from 300-1100 CE compared to the rest of the diagram, due to the higher resolution of this section, which gives the possibility to describe this section in greater detail.

2.5.2.2 Selective diagram

For the selective pollen diagram showing the anthropogenic indicators, the y-axis was adjusted to show the relevant part of the curve, in order to give a better resolution of the Iron Age and the Middle Ages. An interval of 50 years was used for the y-axis. Here, the x-axis was also scaled according to the percentage data of each pollen type. Again, an exaggeration of x20 was applied for the smaller curves. This time, different colours were assigned according to the nature of the anthropogenic indicator. This way, a division was made between indicators of cultivation as opposed to indicators of grazing. Subsequently, the figure was

edited in Adobe Illustrator to manually add the depth markers, as well as the different zones that were previously established in the main diagrams.

2.6 Archaeological data

Archaeological data from Bjørnstad graveyard was used in this study in order to compare archaeological data reflecting the past population of the area to the results of the pollen analysis. The ^{14}C dates retrieved during the excavation in 2017 were analyzed, in order to see during which time period the graveyards surrounding the Bjørnstad farm were in use. In total, 24 ^{14}C dates were retrieved from bone samples taken from the burials and 19 ^{14}C dates were retrieved from samples taken from several features in the soil. These dates were recalibrated for this study, using OxCal version 4.4 (Bronk Ramsey 2009), using the IntCal20 calibration curve (Reimer et al. 2020). Subsequently, they were plotted utilizing the multi-plot function available through OxCal version 4.4 (Bronk Ramsey 2009).

3. Chronology

3.1 Lithology

The peat archive retrieved from the bog reached a depth of 282 cm long and consists of 4 core sections. The measurements of each section are presented in Table 3.

Table 3: The depths in cm for each core

Core number	Depth (cm)
1	0-70
2	70-140
3	140-207
4	207-282

The lithology of the core was described from bottom to top as represented in Figure 12.

<i>HAR18</i>	Upper boundary (cm)	Material	Additional observations: type of boundary, consistency
	0	Light brown peat containing large amounts of plant rests such as roots and some small pieces of wood.	Topsoil; loose, less dense peat. This layer seems quite disturbed.
	10	Dark brown peat containing some large branches or pieces of wood.	This layer contains quite a lot of organic matter and some lighter patches of red grassy peat.
	18	Brown-red grassy peat, containing small grasses and some small wood fragments.	Lighter colour than the previous and subsequent layer.
	26	Dark brown peat, containing less grass.	Few grass fragments; some lighter patches of red grassy peat.
	49	Brown-red grassy peat, containing a large amount of small grasses.	
	70	Light brown-yellow grassy peat layer.	
	86	Dark-brown peat containing large amounts of distinctively large and long grasses, diagonally and vertically crossing the core.	The peat has a light colour compared to deeper parts of the bog: it becomes gradually lighter upwards.
	124	Dark brown peat, less silty texture, less dense.	This layer gradually starts to contain more grasses compared to the lower layers,
	135	Dark brown peat, homogenous; dense.	Contains small pieces of roots, grasses, wood and organic matter;
	202	Dark brown peat.	This section contains some long roots and grasses positioned vertically across the core.
	215	Dark brown peat, containing small pieces of roots, grasses, wood and organic matter; homogenous; dense.	
	232	Dark brown peat; homogenous; dense.	This section contains large amounts of wood.
	242	Dark brown peat, homogenous; dense; silty texture.	Contains occasional small pieces of organic material, such as small patches of wood, some roots and grasses.
	278	Light-grey silty clay; homogenous.	A sharp boundary.
	282	End of coring.	

Figure 12: The lithology of the peat sequence of Haraldstadmyr bog.

The peat profile documented at Haraldstadmyr excavation was described based on several trial pits that were dug. A homogenous, grassy peat layer could be found right below the surface until a depth of approximately 1.20 m. In this layer a large amount of grasses and other plant rests could be seen. From a depth of 1.20-1.30 m large pieces of wood were found. In every pit the tree layer started around the

same depth of 1.20 m. From a depth of 1.30 m onwards large rounded rock fragments were found, which could originate from the glacial debris of the moraine located at the site. Overall, some black patches were found in the bog as well, probably originating from carbonized tree. At the basal part of the sequence the peat was surprisingly dry, possibly as a result of the drainage system which was recently installed. At a depth of 1.70 m the bottom of the bog was reached: the peat was underlain by a grey clay layer. In one of the trial pits a large tree trunk was found at a depth of 1.50 m. The tree trunk was of significant size and of natural origin, without traces of human activity.

3.2 Age-depth model

The age-depth model was generated using the radiocarbon dates shown in Table 4. In this table, for each sample, the minimum and maximum calibrated ages are described, both the BP and BCE/CE systems. In the last column the mean age for each sample is given. The 5 samples retrieved from the core reached a maximum depth of 123.5 cm. As a result, an age-depth model solely based on these radiocarbon ages would be unreliable from depths 123.5 cm until 282 cm.

Therefore, an additional radiocarbon age ‘T?-xxxx’ was used, taken a few years earlier from a different core in Haraldstadmyr bog by K. Griffin, E. Østmo and H. I. Høeg. At their location of coring, this age marked the bottom of the core. Even though this age was retrieved from a different core, it gives an indication of age for the lower part of the Haraldstadmyr peat archive.

Table 4: Table showing the uncalibrated (after Høeg 2018) and calibrated radiocarbon ages for each sample from Haraldstadmyr peat archive .

Lab number	Core depth (cm)	¹⁴ C age BP	Min. age (cal. BP)	Max. age (cal. BP)	Min. age (cal. BCE/CE)	Max. age (cal. BCE/CE)	Mean age (cal. BCE/CE)
Ua-61355	45	866 ± 28	514	754	1436	1196	1260
β-508936	91.5	1040 ± 30	942	1143	1008	807	910
β-508937	102.5	1230 ± 30	1086	1234	864	716	799
β-508938	109.5	1260 ± 30	1183	1286	767	664	708
Ua-61356	123.5	1612 ± 28	1408	1581	542	369	462
N/A	267.5	5010 ± 100	4218	5699	-2268	-3749	-3036

The age-depth model (Figure 13) shows the 6 calibrated radiocarbon dates (BP) listed in Table 4 in blue according to depth. The graph shows an interpolation between the dated samples (in blue), where the red line shows the mean, while the grey lines indicate the minimum and maximum age range. The age-depth model is shown using a ghost graph, where the darker part shows the most frequent interpolation.

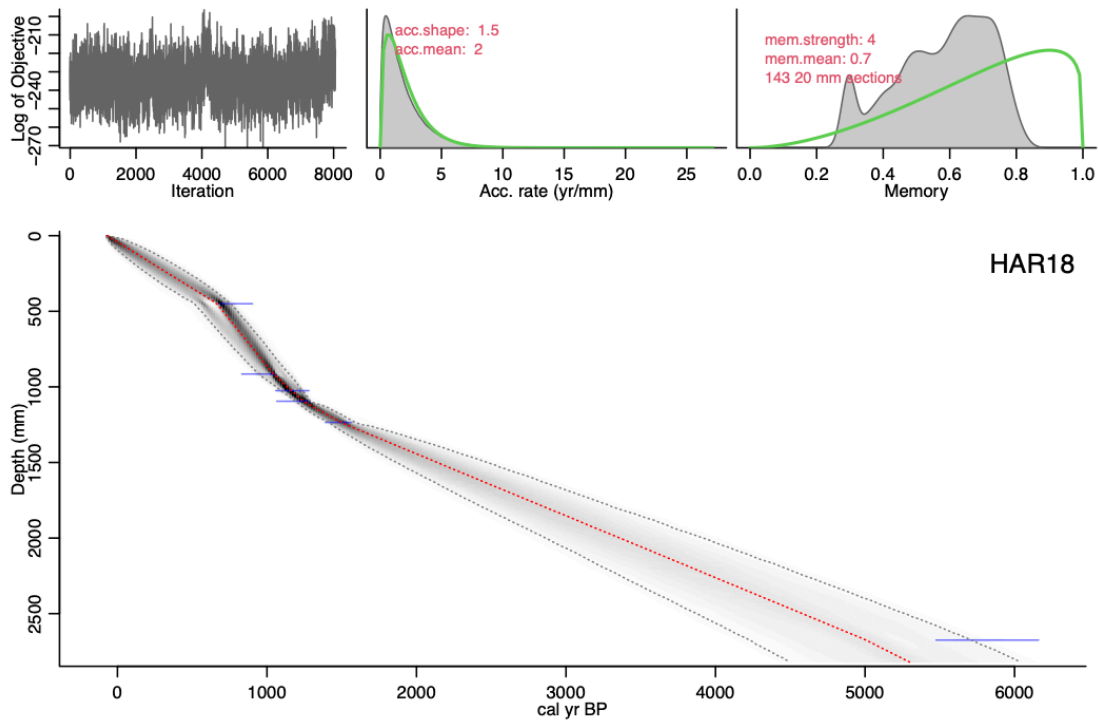


Figure 13: Age-depth model of Haraldstadmyr bog peat sequence showing the calibrated ages according to depth.

According to the age-depth model, the peat profile covers the last 6000 years. The peat accumulation varies throughout the age-depth model. From 6000 cal. BP to 1500 cal. BP the accumulation rate can be described as approximately 0.35 mm/yr. Due to the lack of radiocarbon ages in the basal part of the peat sequence, the ghost graph displays a wide range of possible values. The age-depth model is relatively uncertain in this section; it is possible that the accumulation rate varies to a greater extent throughout this section of the peat sequence than can be noted from the current data. The accumulation increases from 1500 cal. BP to reach 0.64 mm/yr between 1500 cal. BP to 1000 cal. BP. From 1000 cal. BP to c. 690 cal. BP the accumulation rate accelerates to 1.6 mm/yr. Around 690 cal. BP, an abrupt change in the accumulation rate can be seen, resulting in a kink in the graph. From c. 690 cal. BP to 0 cal. the accumulation rate stagnates, resulting in an accumulation rate of approximately 0,63 mm/yr.

4. Pollen record

The pollen diagrams can be found in appendix A.1-A.4. In the pollen diagrams, 9 different zones were defined, as shown in Table 5. The different palynologic zones were identified according to changes in the pollen assemblage. Zone 6 was subdivided into 4 zones: 6A-6D. In this table, mean ages were used to represent the boundaries of the zones.

Table 5: Different zones as defined in the pollen diagrams, with their according ages and depths.

Zone	Age	Depth (cm)
0	3350 BCE - 3200 BCE	282 - 275
1	3200 BCE - 2750 BCE	275 - 255
2	2750 BCE - 2000 BCE	255 - 225
3	2000 BCE - 1100 BCE	225 - 188
4	1100 BCE - 350 BCE	188 - 157
5	350 BCE - 300 CE	157 - 130
6A	300 CE - 450 CE	130 - 124
6B	450 CE - 650 CE	124 - 113
6C	650 CE - 950 CE	113 - 92
6D	950 CE - 1100 CE	92 - 67
7	1100 CE - 1850 CE	67 - 10
8	1850 CE - 2000 CE	10 - 0

4.1 Local vegetation

The pollen diagrams show several transitions in the local vegetation of Haraldstadmyr bog (see appendix A.1-A.4). In zone 0 and 1, the arboreal pollen mostly consist of *Alnus* (appendix A.1). From zone 0 to zone 1 a transition in the pollen assemblage is shown, as a very sudden increase in the amount of *Alnus* pollen occurs, almost doubling the amount of *Alnus* pollen from nearly 50% to 90% (appendix A.1). Noticeable is the occurrence of the green algae *Botryococcus* and *Pediastrum* ($\pm 1-2\%$) contemporary with the presence of the aquatic plants *Typha latifolia*, *Potamogeton* and *Myriophyllum alterniflorum*. These aquatic plants disappear after zone 0, together with the algae *Botryococcus* and *Pediastrum* (appendix A.3). New types of local vegetation appear from zone 1 onwards, such as *Filipendula* and *Apiaceae*, as well as *Dryopteris*. From zone 2 onwards, *Betula* gradually becomes more dominant amongst the tree types in the

pollen record. Spores of *Dryopteris* continue to occur at a stable rate until the start of zone 4.

A new transition can be noted in zone 5, when pollen of the spore plant *Sphagnum* appears (appendix A.2). Throughout the rest of the pollen record, an abundance of *Sphagnum* can be seen, with numbers up to almost 40% of the pollen sum. A contemporary abundance of the heather types *Ericales*, *Empetrum* and *Calluna* can be seen from the same depth onwards (appendix A.1). Other spore plants appearing from zone 5 onwards include *Lycopodium annotinum*, *Gymnocarpium*, *Polypodium* and *Pteridium* (<1%) (appendix A.3). Additionally, microorganisms such as *Helotium*, *Assulina*, *Amphitrema* and *Sordaria* start to appear, namely in zone 6. Aquatic plants seem to return from zone 5 onwards, mostly *Rubus chamaemorus* and *Drosera*, but also *Typha latifolia* and *Menyanthes*. Apart from that, wetland herbs such as *Filipendula*, *Apiaceae* and *Galium* become increasingly abundant from zone 5 onwards (appendix A.3).

In zone 7, an increase in arboreal pollen can be seen. In this zone *Pinus* is the most dominant type of tree pollen. From zone 8 onwards *Betula* pollen seem to increase again, while the amount of *Pinus* pollen decreases (appendix A.1).

4.2 Regional vegetation

For the regional vegetation, the composition as well as the changes in vegetation will be discussed for each zone (see appendix A.1-A.4).

Zone 0: 3350 – 3200 BCE; 282-275 cm

The first zone is marked by a percentage of 88% arboreal pollen (appendix A.1 and A.4). This is a lower number compared to the rest of the diagram. Zone 0 commences with a slight decrease in arboreal pollen, followed by a sharp increase in arboreal pollen from a little before 3250 BCE until 3200 BCE. Pollen of *Alnus* are the most abundant among the tree pollen, with a percentage of 47%, followed by low percentages of *Betula*, *Pinus*, *Corylus*, *Ulmus*, *Quercus*, *Tilia*, *Salix* (\pm 5-10%) and sporadic occurrence of *Populus* and *Prunus/Sorbus* (\pm <1%). Around 3250 BCE a sharp increase in *Alnus* can be seen, in juxtaposition to a decrease in *Betula*, *Pinus*, *Corylus*, *Ulmus*, *Quercus*, *Tilia* and *Salix* (appendix A.1). Amongst the shrubs, small numbers of *Frangula* and *Hedera* shrubs can be seen (<1%).

Additionally, 10% of pollen of *Poaceae* (grasses) occur in this zone, seeing a similar decrease as most of the tree types around 3250 BCE (appendix A.1). Very little amounts of herbs occur throughout this zone (appendix A.2 and A.4). However, small amounts of *Rumex*, *Rumex longifolius* and *Urtica* were found (<1%), as well as small numbers of *Rosaceae*, *Melampyrum*, and *Trifolium*, *Anemone* and *Apiaceae* (appendix A.2). Additionally, some charcoal occurs in zone 0, which seems to disappear for a long period of time after zone 0. The wetland plants and the algae also seem to disappear after zone 0 (appendix A.3).

Zone 1: 3200-2750 BCE; 275-255 cm

Throughout this zone there is a constant percentage of arboreal pollen, around 99 % (appendix A.1). However, this zone sees an incline in *Betula* pollen, as opposed to a decline in *Alnus*. Additionally, a gradual and small incline in *Quercus* and *Tilia* can be seen. Moreover, grasses barely seem to occur in this zone, as well as very few herbs. Some *Rosaceae* remains through this zone, although very little (<1%) (appendix A.2). Additionally, some *Asteraceae* and *Melampyrum* can be found. (<1%). Few pollen of *Rumex* occur, although pollen of *Rumex longifolius* and *Urtica* entirely seem to have disappeared. Other herbs found in this zone are *Filipendula* and *Apiaceae*, which show an increase compared to zone 0, followed by a gradual decrease from 3100 BCE onwards (appendix A.3). Noticeable is a significant increase in *Dryopteris* (spore) from 3200-2900 BCE. Wetland plants, as well as other microorganisms and charcoal remain absent throughout this zone (appendix A.3).

Zone 2: 2750-2000 BCE; 255-225 cm

In zone 2 the amount of *Betula* pollen continues to increase, up to a percentage of 42 around 2150 BCE (appendix A.1). Subsequently, a small decline in *Betula* can be seen until approximately 2000 BCE. The percentages of *Pinus* and *Corylus* seem to be a quite constant continuation of the numbers seen in zone 1. However, *Pinus* shows slight incline around 2650 BCE. The percentage of *Alnus* continues to decrease until 2400 BCE, reaching a percentage of 46, thereby showing a decrease of 43 compared to the beginning of zone 1. From 2400 BCE onwards a slight increase in *Alnus* can be seen up until \pm 2000 BCE. Pollen from *Quercus*

and *Tilia* are present in this zone with percentages varying from 5-10%. Additionally, small numbers of *Fraxinus* and *Salix* occur (<1%) (appendix A.1). Barely any shrubs or grasses occur in this zone (appendix A.4), except for a small number of *Carex* ($\pm 1\%$) (appendix A.1). Small numbers of the herbs *Rumex*, *Artemisia*, *Urtica* and *Plantago lanceolata* occur (appendix A.2). Additionally, the number of *Rosaceae* increases in this zone, especially from 2100 BCE, reaching 1.6% around 2000 BCE. Other herbs found in this zone are *Ranunculus*, *Asteraceae s. Asterioideae*, *Malmpyrum* and *Cornus* (all <1%). The number of *Dryopteris* remains quite constant with a percentage of 10%. However, an increase in *Dryopteris* can be seen from around 2150 BCE into zone 3. No charcoal nor pollen of wetland plants were identified in this zone (appendix A.3).

Zone 3: 2000-1100 BCE; 225-188 cm

In zone 3 the amount of arboreal pollen (AP) is more or less constant. However, the dominant type of tree pollen in zone 3 alternates between *Betula* and *Alnus* (appendix A.1). From 2000 BCE to 1900 BCE *Betula* increases and *Alnus* decreases, followed by an increase in *Alnus* and a decrease in *Betula* from 1900-1650 BCE. From 1650-1400 BCE *Alnus* decreases and *Betula* increases again, followed by a decline in *Betula* and an incline in *Alnus* up to 1150 BCE. The percentages of *Pinus* and *Corylus* stay more or less constant throughout the zone. *Fraxinus* slightly increases in this zone, while *Quercus*, *Tilia* and *Salix* maintain their numbers as a continuation of zone 2. Again, very few to zero pollen of shrubs and grasses, sedges or rushes occur in this zone (appendix A.4). Herbs occurring in zone 3 include *Chenopodiaceae*, *Plantago lanceolata*, *Hordeum*, *Rosaceae*, *Caryophyllaceae*, *Filipendula* and *Apiaceae*. An increase of *Filipendula* can be seen from approximately 1300 BCE onwards. *Rosaceae* declines gradually in zone 3 (appendix A.2). This zone contains the greatest amount of *Dryopteris* spores in the pollen record, as two peaks occur at 1850 BCE and 1150 BCE. After zone 3, *Dryopteris* seems to drastically decrease, from almost 20% to less than 1%. It remains a low number for the rest of the pollen record (appendix A.3). Additionally, a reappearance of charcoal particles in the samples can be seen around 1450 BCE.

Zone 4: 1100-350 BCE; 188-157 cm

In zone 4 an increase in *Betula* can be seen, compensated by a decrease in *Alnus*. The amount of *Pinus* pollen remains roughly the same as before. In this zone small numbers of tree pollen from *Fagus*, *Ulmus*, *Quercus*, *Tilia*, *Fraxinus*, *Hedera* and *Salix* occur, as well as a small number of the shrub *Hedera*. Some grasses seem to return as well, as a low number of *Elymus* appears in this zone (appendix A.1). Additionally, more herbs seem to occur in zone 4 as compared to the previous zones (appendix A.4), such as *Rumex*, *Rumex longifolius*, *Artemisia*, *Chenopodiaceae*, *Urtica*, *Plantago lanceolata*, *Hordeum*, *Avena*, *Rosaceae*, *Ranunculus*, *Caryophyllaceae*, *Asteraceae s. Cichorioideae*, *Melampyrum*, *Cornus*, *Hypericum* (appendix A.2), *Filipendula* and *Galium* (appendix A.3). Spores of *Lycopodium annotinum* occur, as well as a small number of *Dryopteris*. Noticeable is the appearance of *Sordaria* in this zone, as well as a significant peak in charcoals (appendix A.3).

Zone 5: 350 BCE- 300 CE; 157-130 cm

This zone sees a decrease in *Betula*, except for a spike halfway through the zone, correlating with a sharp decrease in *Alnus*. *Pinus* seems to show a gradual, slight increase, with an average pollen percentage around 10%. *Corylus* seems to be constant throughout the zone. Other tree types occurring in this zone are *Fagus*, *Populus*, *Ulmus*, *Quercus*, *Tilia*, *Fraxinus*, *Salix*, *Prunus/Sorbus* (appendix A.1). A significant transition can be seen in the occurrence of dwarf shrubs (appendix A.1 and A.4). The heather types *Ericales*, *Empetrum* and *Calluna* appear for the first time in the pollen record, with significant numbers, especially *Calluna* (almost up to 40%). A similar transition can be seen in the abundance of grasses. Especially *Carex* and *Poaceae* show a significant increase in percentages. More herbs occur compared to the previous period. The numbers of *Rumex*, *Artemisia*, *Chenopodiaceae*, *Urtica*, *Plantago major* and *Plantago lanceolata* sharply increase, especially near the end of the zone (appendix A.2). Other herbs occurring in this diagram are *Rumex longifolius*, *Avena* (near the end of the zone), *Rosaceae*, *Potentilla*, *Ranunculus*, *Caryophyllaceae*, *Asteraceae s. Cichorioideae*, *Melampyrum*, *Chrysanthemum*, *Epilobium*, *Hypericum*, *Scrophulariaceae*, *Stachys*, *Persicaria*, *Filipendula* (with a very constant number throughout the entire zone), *Apiaceae* and *Galium*.

In this zone the aquatic plant *Rubus chamaemorus* occurs, which is the first aquatic plant to appear in the pollen record. Noticeable is the large amount of *Sphagnum* throughout the zone, which seems to commence in zone 5. Overall, many spore plants occur, such as *Lycopodium annotinum*, *Dryopteris*, *Gymnocarpium*, *Polypodium* and *Pteridium* (appendix A.3). Additionally, the microorganisms *Helotium* and *Sordaria* occur in this zone. Finally, a large increase in charcoal particles can be seen in zone 5, after a period of less charcoal in between zone 4 and 5 (appendix A.3).

Zone 6A-6D: 300-1100 CE, 130-67 cm

Zone 6 has been subdivided into 4 different zones, due to the high resolution of pollen analysis in this zone. The composition of tree pollen varies throughout the different subzones, however, noticeable is a significant increase in *Betula* in zone 6B and 6D (appendix A.1). In zone 6A, the amount of arboreal pollen overall seems to be lower, as opposed to the increase in arboreal pollen in zone 6B and 6D. Other tree pollen occurring in zone 6 include *Picea*, which appears from subzone 6B onwards, as well as *Fagus*, *Populus*, *Carpinus*, *Quercus*, *Fraxinus*, *Salix* and *Juniperus*, primarily in subzone 6C. The dwarf shrubs *Myrica*, *Ericales*, *Empetrum* and *Calluna* remain present throughout the zone, despite a temporary disappearance of *Ericales* and *Empetrum* in subzone 6B. Zone 6 is especially marked for the large amount of grasses, sedges and rushes occurring throughout the zone, such as *Carex*, *Eriophorum*, *Scirpus*, *Poaceae* and *Elymus*, where again zone 6B and 6D show a decrease in *Carex*, *Eriophorum* and *Scirpus* (appendix A.1). A large variety of herbs occurs throughout zone 6 (appendix A.2). Overall, zone 6B and 6D show a decrease in herbs, as opposed to the extensive number of herbs in especially zone 6C, but also zone 6A (appendix A.4). Primarily the herbs *Rumex*, *Artemisa*, *Chenopodiaceae*, *Urtica*, *Humulus/Cannabis*, *Plantago major*, *Plantago lanceolata*, *Rosaceae*, *Ranunculus* and the cereals *Hordeum Triticum*, *Avena*, *Secale* seem to peak in both subzone 6A and 6C (appendix A.2). In subzone 6C a pattern of two high peaks can be seen amongst the cereals, alternated by lower numbers. Furthermore, the aquatic *Drosera* occurs in zone 6B and C, as well as a small amount of *Lythrum* in zone 6B. A small amount of *Rubus chamaemorus* occurs in zone 6A and 6C. Relatively high amounts of spore plants occur throughout zone 6C, especially spores of *Sphagnum* (appendix A.3).

Noticeable is the appearance of the microorganisms *Helotium*, *Assulina*, *Amphitrema* and *Sordaria*. The number of charcoal particles varies throughout zone 6, showing a higher amount of charcoal in zone 6B and 6C as compared to zone 6A and zone 6D. Subzone 6D shows an especially low amount of charcoal particles when compared to the other subzones, as a result of a significant sharp and sudden decline in the amount of charcoal right after zone 6C (appendix A.3).

Zone 7: 1100-1850 CE, 67-10 cm

In this zone the arboreal pollen increase (appendix A.1 and A.4). This increase seems to start primarily with an increase in pollen of *Pinus* as opposed to a decrease in pollen of *Betula*, followed by a subsequent gradual increase in *Betula*. In this zone the heather types *Ericales*, *Empetrum* and *Calluna* persist to occur (appendix A.1). However, the grasses seem to disappear, except for a low number of *Poaceae*. After disappearing mostly in subzone 6D, some of the herbs gradually return, although in lower numbers compared to subzone 6C. Amongst these are *Rumex*, *Artemisia*, *Humulus/Cannabis*, *Hordeum*, *Triticum*, *Avena*, *Secale*, *Rosaceae*, *Ranunculus*, *Melampyrum*, *Lotus*, *Trifolium* and *Hypericum* (appendix A.2). Other herbs such as *Filipendula*, *Apaciaceae* and *Galium* seem to be absent in zone 7 (appendix A.3). Zone 7 shows some aquatic plants, namely *Rubus chamaemorus*, and some of the spores. *Sphagnum* remains dominant throughout zone 7 as well. The microorganisms seen in zone 6 seem to remain absent in zone 7. Furthermore, the amount of charcoal particles is particularly low throughout the entire zone, when compared to the previous zones (appendix A.3).

Zone 8: 1850-2000 CE, 10-0 cm

The last zone sees a decrease in arboreal pollen (appendix A.1 and A.4). However, *Betula* increases as opposed to a decrease in *Pinus*. Many of the tree types seen in previous zones remain fairly absent throughout this last zone, except for pollen of *Alnus*, *Picea*, *Salix* and *Prunus/Sorbus* (appendix A.1). The grasses remain absent throughout the zone, following the same pattern as seen in zone 7 (appendix A.4). Amongst the herbs an increase can be seen in *Rumex* and *Artemisia*. Additionally, the cereals *Hordeum*, *Triticum*, *Avena* and *Secale* seem to have returned and show a slight increase in comparison with zone 7 (appendix

A.2). Other herbs noteworthy of mentioning in this zone are *Rosaceae*, *Ranunculus*, *Melampyrum* and *Chrysanthemum*, *Apiaceae* which all show considerable amount of pollen when compared to the previous zone. The aquatic plant *Typha latifolia* appears, as well as low amounts of *Menyanthes* and *Rubus chamaemorus*. Amongst the spores, *Sphagnum* and *Dryopteris* are the most prominent (appendix A.3). The amount of charcoal particles remains low, although a peak can be seen around the boundary from zone 7 to zone 8.

5. Archaeological data

5.1 Finds in the area

Numerous excavations took place located along the Raet. Approximately 140 structures were excavated, including a ship excavation, three coffin burials from the Early Iron Age, a grave from the Roman times, and remains of a cultivation layer (Iversen 2017, 2-4). In addition, 124 settlement traces were found, which included 54 post holes, a fireplace, 10 cooking pits, 5 pits which could be interpreted as ovens and 41 burials. In total, 25 samples were dated, showing 8 of the samples originated from the Early Bronze age – pre-Roman Iron age and 10 of the samples were dated to the Roman period – Viking period (Iversen 2017, 2-4). In addition to that, one coffin burial was dated to Roman period based on reused material, and one cooking pit was dated to the late Bronze age. At the excavation site of Bjørnstad, most finds were found to origin from the Early Iron age, most likely the pre-Roman Iron Age. Together, these dates show continuous activity in the area over more than 1000 years (Iversen 2017, 2-4).

5.2 Burials along the Raet in Vestfold district

A study by Solheim and Iversen (2019) utilized a large radiocarbon dataset from burial graves located alongside the Raet in Vestfold district in order to reconstruct the past population size and human activity through time (Solheim and Iversen 2019, 423). In their study 855 radiocarbon determinations were used as a proxy for significant changes in activity through time. As a result, they found a steady increase in dates and human population or activity from 2000 BCE onwards (Solheim and Iversen 2019, 429). Subsequently, a significant increase was found during both the pre-Roman Period and the Roman Period (500 BCE-400 CE), followed by a steady, but fluctuating demographic decrease from 400 CE to 550 CE. From 550 CE to 800 CE a significant decrease was (Solheim and Iversen 2019, 429-30) found, which could be recognized as the well-studied mid-6th-century crisis that occurred across Europe (Solheim and Iversen 2019, 423). In the medieval period, from 1000-1500 CE, fewer radiocarbon dates occurred, although dates from medieval towns were not systematically collected during their study (Solheim and Iversen 2019, 427).

5.3 Burials along the Raet in Østfold district

In total, close to a thousand graves are known from Østfold. From the farms located at Store Tuen and Grålum, several were dated to the pre-Roman Iron Age, some containing metal objects of iron and bronze. The radiocarbon dated burials from the Bjørnstad excavation show that the burial site at Bjørnstad has been in continuous use for at least 700 years, from the Roman Iron Age to the Merovingian period. It is possible that the burial site represents an early phase in the development of a larger farm burial ground, as it seems like people, most likely the farmers from Bjørnstad, have been buried in the nearby area over a long period of time (Iversen 2017). The results from the osteological analysis of the excavation show that the burial ground was in use from at least the Roman time to the Viking Age. An even distribution of the sexes was found, which could be an indicator that the burial site served as a cemetery for the people living at the Bjørnstad farm. The inventory of the graves varied from more rich equipped graves to more simple ones (Iversen 2017, 2-4).

5.4 Radiocarbon dates from Bjørnstad burial site

The 19 calibrated dates taken from different structures from the excavation at Bjørnstad are listed in the table below (Table 6). The different types of organic material that were sent in for dating are listed in the table: the samples originated from different tree species. However, it was not mentioned which part of the tree was sent in for radiocarbon dating. The dates ranged from 778 BC to 1800 CE, with a probability of 95,4%. The uncalibrated dates can be found in appendix B.

Table 6: Table showing the calibrated dates of different structures from Bjørnstad burial site (source?).

Sample number	Find number	Type of structure	Type of sample	Min. age cal. - max. age cal. (BCE/CE)	Lab-no.
5035	102	Waste pit	<i>Acer platanoides, Alnus, Betula, Quercus</i>	129 - 352	LuS-13372
5033	138	Cooking pit	<i>Pinus, Quercus</i>	246 - 432	LuS-13371
5083	162	Waste pit	<i>Pinus</i>	1328 - 1456	LuS-13379
5109	176	Holloway	<i>Picea abies, Betula, Pinus, Salix caprea</i>	1054 - 1273	LuS-13380
5062	179	Waste pit	<i>Picea abies, undefined deciduous tree</i>	1500 - 1800	LuS-13374
5082	180	Holloway	<i>Alnus, Betula, Salix caprea, Populus tremula, Corylus</i>	425 - 605	LuS-13378
5074	182	Cultivation layer	<i>Alnus, Betula</i>	-749 - -393	LuS-13377
5065	183	Ring ditch	<i>Pinus, Alnus or Betula</i>	1038 - 1212	LuS-13375
5113	190	Waste pit	<i>Pinus</i>	1054 - 1273	LuS-13381
5030	197A	Cooking pit	<i>Alnus, Betula</i>	-772 - -418	LuS-13369

5031	197B	Cooking pit	<i>Alnus, Betula</i>	-775	-	-422	LuS-13370
5149	212	Ditch	<i>Pinus, Picea abies</i>	1288	-	1398	LuS-13384
5150	213	Ditch	<i>Betula, Pinus</i>	1511	-	... (out of range)	LuS-13385
5151	214	Ditch	<i>Pinus, Picea abies</i>	1433	-	1632	LuS-13386
5040	245	Circular ditch	<i>Pinus, undefined coniferous tree</i>	1646	-	... (out of range)	LuS-13373
5134	149	Unknown structure	<i>Alnus, Corylus</i>	-756	-	-408	LuS-13383
5026	251	Coffin	<i>Betula, Salix caprea</i>	-753	-	-403	LuS-13368
5127	125	Unknown structure	<i>Betula, Quercus, Alnus</i>	-778	-	-423	LuS-13382
5073	263	Posthole	<i>Betula, Corylus, Quercus</i>	414	-	567	LuS-13376

In the following plot (Figure 14) the calibrated dates of the structures are displayed according to time. For each structure listed to the left, a probability distribution for the dating is shown in grey. A large spread in dating between the features can be seen, covering a time period of approximately 2600 years. The more recent dates, however, can suggest a possible disturbance of the subsoil.

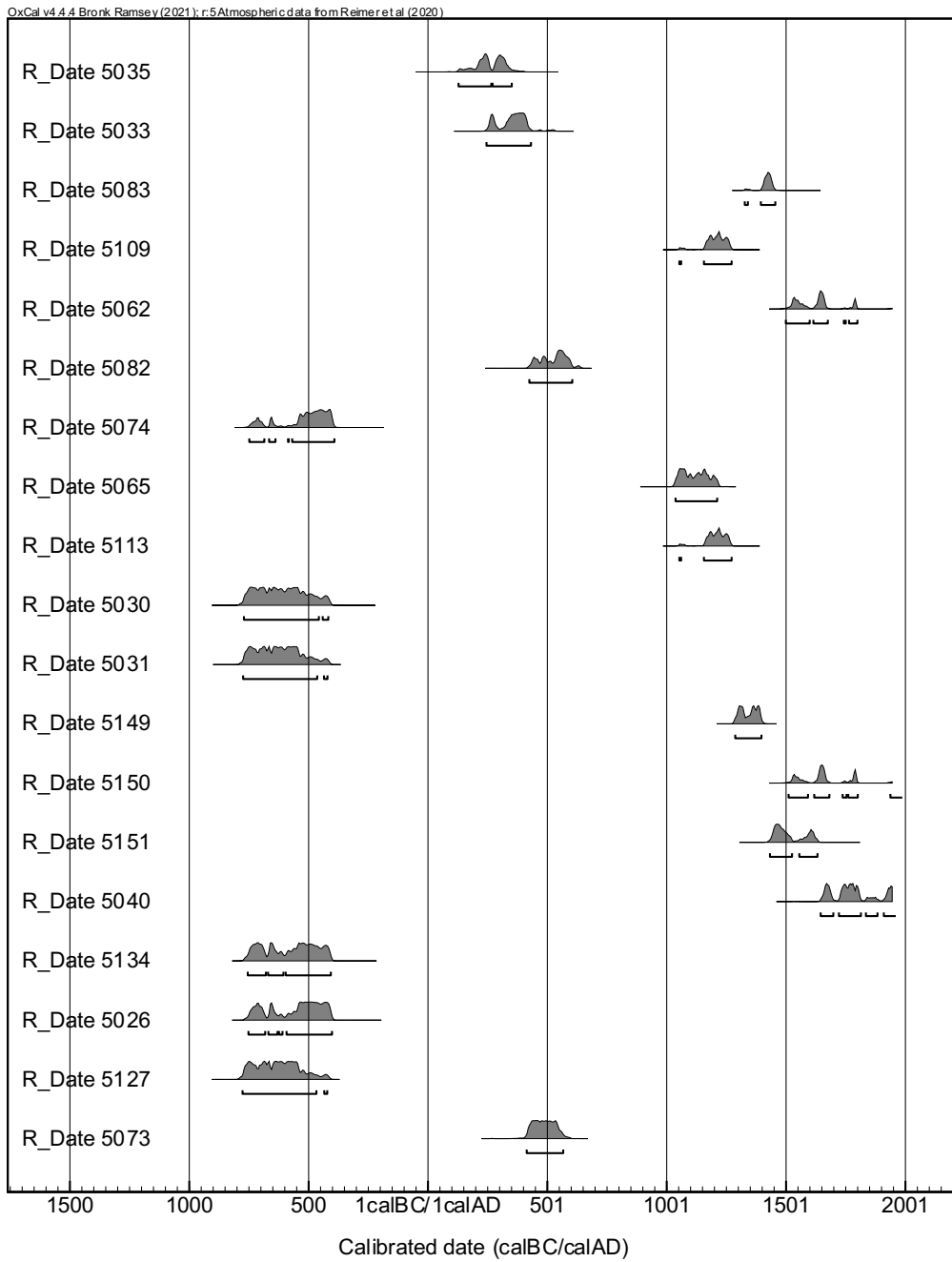


Figure 14: Plot showing the distribution of the calibrated radiocarbon dates from the structures at Bjørnstad burial site according to time, where the probability distribution for each date is displayed in grey.

The calibrated radiocarbon dates from the burials at Bjørnstad are shown in Table 7. The dates ranged from 172 cal. BC to 986 cal. CE, with a probability of 95.4%. The uncalibrated dates can be found in appendix B.

Table 7: Table showing the calibrated radiocarbon dates from the burials located at Bjørnstad burial site (source).

Sample number	Find number	Type of feature	Type of sample	Min. age cal. - max. age cal. (BCE/CE)	Lab-no.
5001	109	Burial	Human bone	236 - 412	LuS-12917
5002	115	Burial	Human	605 - 775	LuS-12918
5003	120	Burial	Human	-36 - 212	LuS-12919
5004	123	Burial	Human	231 - 406	LuS-12920
5005	137	Burial	Human	772 - 986	LuS-12921
5006	141	Burial	Human	365 - 553	LuS-12922
5007	156	Burial	Human	424 - 590	LuS-12923
5008	157	Burial	Human	246 - 432	LuS-12924
5020	206	Burial	Human	663 - 877	LuS-12925
5032	143	Burial	Human	246 - 531	LuS-12926
5049	141	Burial	Human	121 - 354	LuS-12927
5050	139	Burial	Human	81 - 335	LuS-12928
5051	260	Burial	Human	262 - 540	LuS-12929
5057	115	Burial	Human	256 - 537	LuS-12930
5059	133	Burial	Human	241 - 407	LuS-12931
5061	123	Burial	Human	247 - 533	LuS-12932
5066	262	Burial	Human	426 - 596	LuS-12933
5067	156	Burial	Human	436 - 648	LuS-12934
5081	271	Burial	Human	242 - 408	LuS-12935
5096	272	Soil mark	Human	249 - 531	LuS-12936
5101	157	Burial	Human	260 - 540	LuS-12937
5111	157	Burial	Human	172 - 76	LuS-12938
5137	218	Burial	Human	-93 - 127	LuS-12939
5155	279	Burial	Human	172 - 60	LuS-12940

The following plots (Figure 15 and 16) show the burial dates according to time. The probability distribution of the dates is displayed in grey. It can be noted that most of the dates occurring in more or less the same range of age, between 0 and

550 CE, although some outliers occur. In total, the ages cover a time period of approximately 1150 years.

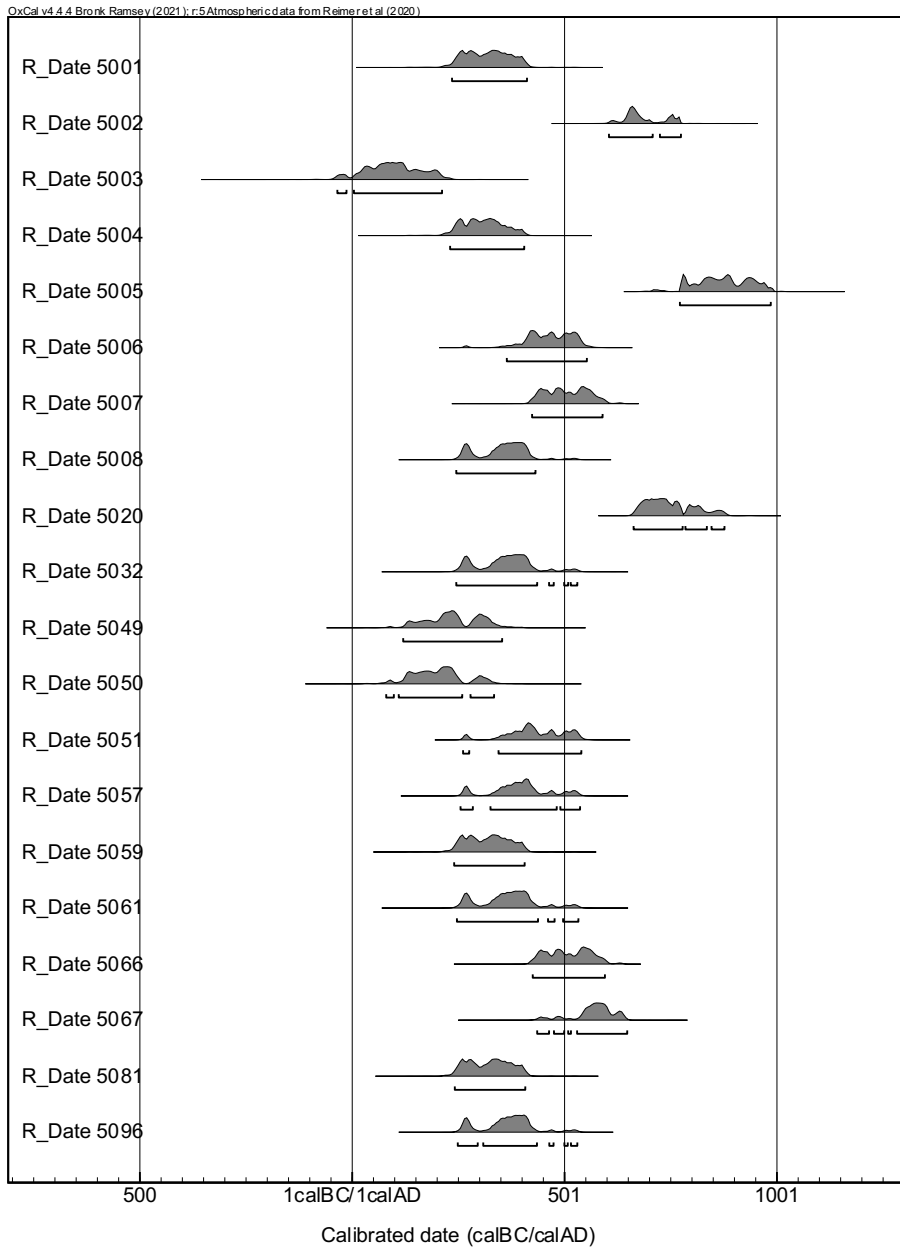


Figure 15: Plot displaying the distribution of the calibrated radiocarbon dates from the burials located at Bjørnstad burial site according to time, where the probability distribution for each date is depicted in grey.

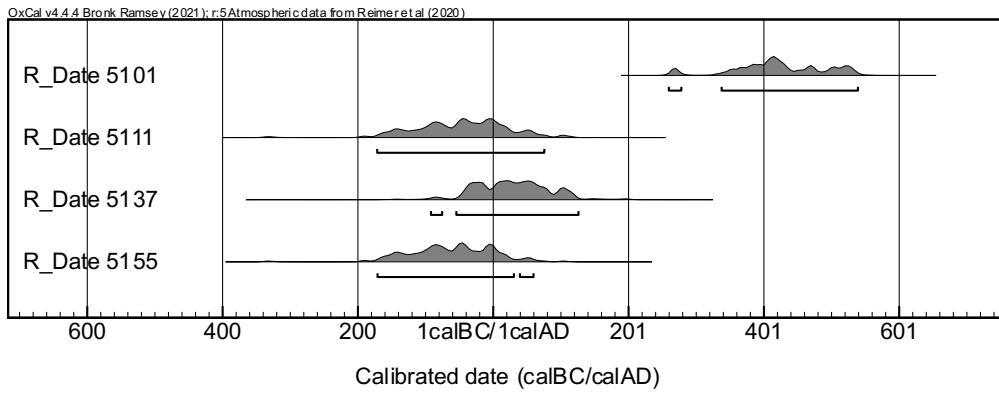


Figure 16: Plot displaying the distribution of the calibrated radiocarbon dates from the burials located at Bjørnstad burial site according to time, where the probability distribution for each date is depicted in grey.

In Table 8 and Figure 17, the number of dated graves found at Bjørnstad burial site are categorized into different periods in time, ranging from the Pre-roman Iron Age to the Viking period. These numbers are based on the median calibrated ages. The six different periods were distinguished by using an interval of 200 years.

Table 8: Table showing the number of dated graves found at Bjørnstad burial site for each period in time, ranging from the Pre-roman Iron Age to the Viking period, using an interval of 200 years.

Period in time	Min. age BCE/CE	Max. age CE	Number of dated graves
Pre-roman Iron age	-200	0	2
Early Roman Iron Age	0	200	2
Late Roman Iron Age	200	400	11
Migration period	400	600	6
Merovingian period	600	800	2
Viking period	800	1000	1

The dates span from the pre-roman Iron Age to the Viking Period. The majority of the dates, 15 out of 24, date from before 550 CE (Table 8; Figure 17). From these 15 graves, the majority was dated to the Late Roman Iron Age. Subsequently, 6 of the graves were dated to the Migration period, occurring around 550 CE. After the Migration period, a decrease in the number of dated graves could be seen. In total, 3 graves could be placed in the Merovingian period and the Viking period.

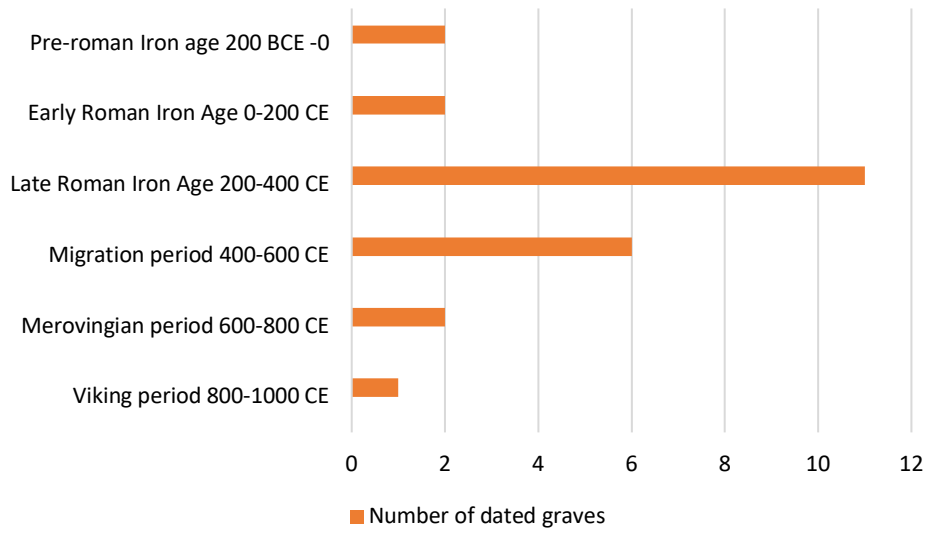


Figure 17: Graph showing the distribution of the number of dated graves found at Bjørnstad burial site categorized into different periods in time, using an interval of 200 years.

6. Discussion

6.1 Development of the local vegetation and environment of Haraldstadmyr bog

The local vegetation and environment of Haraldstadmyr bog was reconstructed through time by interpreting the pollen record. Two distinct transitions seem to occur in the local vegetation, distinguishing three different paleoenvironments from another. The changes seen in the pollen assemblage seem to correspond with changes found in the lithology of the peat sequence. The three different paleoenvironments will be discussed from bottom to top.

First of all, in zone 0, the occurrence of the aquatic plants suggests a wet environment. *Typha latifolia* usually grows in flooded areas, and *Potamogeton* is known as a freshwater aquatic plant. The contemporary occurrence of the green algae *Botryococcus* and *Pediastrum* supports this interpretation, as both algae are usually found in freshwater environments. *Botryococcus* is commonly found in temperate freshwater lakes, although it can occasionally occur in estuaries and fjord. The presence of these aquatic plants and green algae in zone 0 suggest a freshwater environment, such as a lake. Additionally, *Alnus* represents the majority of the arboreal pollen. *Alnus* usually finds its natural habitat in moist ground near rivers, ponds and lakes. After zone 0, these aquatic plants disappear simultaneously with the green algae, announcing a sharp transition into zone 1. These findings correlate with transitions seen in the lithology of the peat sequence (Figure 12), where the basal part of the peat sequence (282-277 cm) represents a clay layer, followed by a sharp transition to a dark brown homogenous peat layer. These results suggest a lake environment from 282 cm – 277 cm, which according to the age-depth model corresponds to the period 3350 – 3200 BCE (Figure 13). These findings are in line with the expected formational process of hydrosereal succession, where a raised bog usually starts as a lake, gradually developing into a fen (Figure 18) or bog (Figure 9).

Subsequently, in zone 1 the aquatic plants and green algae disappear. The lake environment seems to develop into a fen, showing an abundance of *Alnus* pollen and the appearance of *Salix* pollen from zone 1 up until zone 4, dated from 3200 to 350 BCE. The local vegetation of fens usually includes small trees such as

willow (*Salix*) and alder (*Alnus*) (Figure 18). Fens are often minerotrophic as opposed to poor fens and bogs which are often ombrotrophic. The arboreal pollen of zones 1-4 are dominated by both *Alnus* and *Betula*, suggesting minerotrophic conditions during these zones (O'Reilly et al. 2014, 16). Additionally, zones 1-4 contain an abundance of *Dryopteris* (fern). Ferns are known to inhabit warm, damp areas, often occurring in open bogs or marshes (Mickel 2020). The absence of *Sphagnum* mosses during these zone supports the hypothesis of a fen environment from 3200 to 350 BCE.



Figure 18: Picture showing the local vegetation of a fen, such as small trees of the species *Salix* and *Alder* (Kruusamägi 2015).

A second transition can be seen around a depth of 150 cm, between zone 4 and zone 5, when the spore plant *Sphagnum* becomes one of the most abundant species in the pollen assemblage, accompanied by the heather types *Ericales*, *Empetrum* and *Calluna*. The appearance of *Sphagnum* and its marked abundance from zone 5 onwards marks a clear fen-to-bog transition in the pollen record. According to the age-depth model this transition occurs around 350 BCE. From then onwards, the abundance of *Sphagnum*, *Ericales*, *Empetrum* and *Calluna* indicate that Haraldstadmyr could be identified as a raised bog predominantly

formed by *Sphagnum*; in other words: a sphagnum bog (Figure 19). This transition can also be recognized in the lithology of the peat sequence: the lithology changes from a dense homogenous dark brown peat in the lower part of the core to a lighter, less dense peat containing large amounts of grasses and *Sphagnum* in the upper part of the core.



Figure 19: Picture showing the local vegetation commonly found at raised bogs, such as the heather types *Ericales*, *Empetrum* and *Calluna* (<http://raisedbogs.ie/>).

6.2 Development of the regional vegetation and environment

The abundance of pollen of trees indicates that the region of Haraldstadmyr was densely forested up until 1200 BCE. From 1200 BCE a decline in *Alnus* pollen can be seen, followed by a subsequent increase in *Filipendula* from 1300 BCE onwards (appendix A.1; A.3; A.4). These changes suggest the gradual disappearance of Alder forests (*Alnus*) in wet valleys or areas, leading to the emergence of pasture grounds and the growth of *Filipendula*. A decline in arboreal pollen from 1200 to 800 BCE, coinciding with a relative increase in charcoal particles supports the interpretation of a clearance of woodlands in the region from 1200 to 800 BCE. During this period, an increase in herbaceous pollen and pollen of grasses, sedges and rushes can be seen. An increase of *Rumex*, *Rumex longifollus*, *Artemisia*, *Chenopodiaceae*, *Urtica*, *Plantago lanceolata*, *Hordeum*, *Avena* in the pollen assemblage suggests a period of farming and cultivation from 1200 to 800 BCE (appendix A.2 and A.5). Subsequently, from 800 BCE onwards, there is an increase of arboreal pollen again where percentages reach close to a 100%, suggesting densely forested areas in the region. Thus, a reforestation of the region seems to take place. A new transition, however, occurs around 350 BCE, when a rapid decline in

arboreal pollen suggests a secondary clearance of the woodland in the region. The decline in arboreal pollen coincides with a contemporary incline in charcoal and *Pteridium*, suggesting more fire activity. Additionally, a significant incline in pollen of grasses and herbs can be recognized, which serves as an indicator for a more open landscape in the region (appendix A.4). An increase can be seen in the herbs *Rumex*, *Artemisia*, *Chenopodiaceae*, *Urtica*, *Cannabis*, *Plantago major*, *Plantago lanceolata*, *Trifolium*, the cereals *Hordeum*, *Triticum*, *Avena*, *Secale* and in spores of *Sordaria*, leading to the interpretation that from 350 BCE onwards the woodlands were cleared in order to establish fields for cultivational purposes and husbandry (appendix A.5). Compared to the 1200-800 BCE suggested period of cultivation, the numbers of herbaceous plants and pollen of grasses, sedges and rushes are much higher during this new period commencing around 350 BCE (appendix A.4). Thus, cultivation seemed to be occurring to a much greater extent compared to the period of 1200-800 BCE. A new transition in the regional vegetation occurs around 950 CE, when an initial increase in *Betula* is followed by an increase in *Pinus* and *Juniperus* pollen, resulting in a significant incline in arboreal pollen, which can be interpreted as a reforestation of the area (appendix A.4). This incline coincides with a decline in crop plants, *Sordaria* and grasses, suggesting a cease in cultivation and animal husbandry.

6.3 Evolution of farming activities from the Early Iron Age to the Medieval Period

6.3.1 A new onset of farming in the Early Iron Age

Around 350 BCE (beginning of zone 5) a marked decline in arboreal pollen, coinciding with an incline in anthropogenic indicators and grasses, suggests a new onset of farming in the Early Iron Age, after a period of reforestation and a decline in cultivation from 800 BCE to 350 BCE (appendix A.5). The presence of farming activity can be confirmed by several dated archaeological finds from the area that suggested farming activities, such as two cultivation layers, two possible ovens, two post holes and a fireplace (Table 6). These finds were dated to the pre-Roman Iron Age: in other words, the Early Iron Age. Anthropogenic indicators such as charcoal, *Hordeum*, *Rumex*, *Artemisia*, *Chenopodiaceae*, *Urtica*, *Plantago major*, *Pteridium* and *Plantago lanceolata* show signs of cultivation and animal

husbandry from 350 BCE onwards. However, farming activities seem to peak later on between 300 and 950 CE (zone 6) (appendix A.5). The pollen record shows an alternation of different types of farming. From 350 BCE to 300 CE (zone 5) pastoral activity seems to be most prominent, indicated by the presence of *Rumex*, *Artemisia*, *Chenopodiaceae*, *Urtica*, *Plantago major*, *Plantago lanceolata* and ascospores of *Sordaria* (appendix A.5).

At Bjørnstad burial site a cultivation layer was dated to 749-393 cal. BCE. The timing of the new onset of farming activities around 350 BCE could correspond with the date of the cultivation layer, although it would place the onset of cultivation around this time slightly earlier than the pollen analysis. Pollen of *Cannabis* were found in the pollen record from 450 BCE onwards, after which other anthropogenic indicators followed in 350 BCE (appendix A.5). Thus, the dated cultivation layer possibly corresponds with the small number of *Cannabis* pollen found in the pollen assemblage from 450-200 BCE.

6.3.2 Transitions from pastoral to mixed farming from the Late Iron Age into the Viking Age

From 300 CE onwards more cultivation seems to take place next to the previously established grazing activities (appendix A.5). Due to the high resolution of the pollen analysis as from 300-1000 CE (zone 6) as described in chapter 2, several short alternations in agricultural activities could be distinguished within this period. From 300 to 950 CE (zone 6), the farming activities seem to alternate between mixed farming, which can be described as a combination of cultivation and grazing activities, and pastoral farming, which primarily consists out of grazing activities (appendix A.5). Additionally, periods where more farming activities seemed to take place were alternated with periods of less agricultural activity. From 300-450 CE (zone 6A) indicators of both cultivation (i.e. *Hordeum*, *Triticum* and *Secale*) and grazing activities (i.e. *Plantago lanceolata*, *Rumex*, *Rumex longifolius*, *Artemisia*, *Chenopodiaceae*, *Urtica* and ascospores of *Sordaria*) are presented in the pollen record (appendix A.5).

A transition occurs in zone 6B, around 450 CE, when an incline in arboreal pollen, primarily due to increase in *Betula* pollen, suggests a period of increased

forestation (appendix A.5). *Betula* is a pioneer species and is commonly one of the first trees to settle during the natural colonization of a landscape, for example after a glacial retreat or an abandonment of the land (Fischer et al. 2002, 17). In addition, a decrease can be seen in the cereal crops *Hordeum*, *Triticum* and *Secale*, which remain relatively absent from 450 until 650 CE (appendix A.5). Some grazing seems to continue throughout the period of 450-650 CE (zone 6B), suggested by the presence of *Rumex* and *Artemisia*. However, also the pollen types *Chenopodiaceae*, *Urtica* and ascospores of *Sordaria* remain relatively absent throughout this period (appendix A.5). This decrease in anthropogenic indicators, coinciding with an increase in *Betula* and a decrease in dwarf shrubs and grasses, indicates a period of less agricultural activity, or perhaps even an abandonment around the 6th century CE, from 450 to 650 CE (appendix A.5).

After 650 CE a rich period in agricultural activities seems to occur up until 950 CE (zone 6C, appendix A.5). This zone shows the highest peaks of the cereal crops *Hordeum*, *Triticum*, *Avena* and *Secale*, as well as the highest number of *Cannabis* pollen so far. The zone can be subdivided in four parts (appendix A.5). First, the period from 650 to 750 CE is characterized by an abundance of indicators of grazing, such as *Rumex*, *Artemisia*, *Chenopodiaceae* and *Sordaria*. However, also pollen of *Cannabis* can be found during this period. Subsequently, from 750-825 CE distinct peaks in the pollen record can be seen for all four cereal crops *Hordeum*, *Triticum*, *Avena* and *Secane*, as well as for the indicators of grazing, especially *Sordaria* (appendix A.5). Additionally, a decline in arboreal pollen can be seen. Thus, 750-825 CE can be interpreted as a period of mixed farming. This period is then followed by an alternation with less cultivation of crops from 825-900 CE signaled by an incline in arboreal pollen around 825 CE and an abrupt decrease in cereal crops as well as *Cannabis*. However, grazing activities seem to remain active during this period, signaled by an increase in *Rumex*, *Artemisia* and especially *Sordaria* (appendix A.5). From 900-950 CE a significant increase in cereal crops and an abrupt decrease in arboreal pollen indicates the occurrence of another period of high cultivational activity. Noticeable is a significant high peak in *Sordaria*, supported by an abundance in *Rumex* and *Artemisa*, suggesting grazing activities throughout this period (appendix A.5). As a result, 900-950 CE can be interpreted as a period of mixed

farming. This way, the period from 650 to 950 CE is characterized by an alternation of mixed farming and pastoral farming.

The dates of the archaeological burial site show continuous habitation from the Pre-roman Age into the Early Viking period (approx. 172 BCE to 986 CE), corresponding with the presence of farming activity signaled in the pollen record. By interpreting the numbers of graves occurring in each period of time an idea could be formed on the differences in size of the population living at the farm and the land use intensity in the local area through time. Most burial dates occurred in the Roman Iron Age, up until 400 CE. This result is in line with the study performed by Solheim and Iversen in 2019, where they found a significant increase in radiocarbon dates from burial graves in the Roman Period up until 400 CE. In the Migration period, from 400 to 600 CE, a slight decrease in the number of burial dates could be seen. Subsequently, in the Merovingian period from 600-800 CE, the number of burial graves showed a significant decline. These results correspond with the results from the pollen record, which indicates a decline in human activity in the period 450-650 CE, as well as a decline in cultivation in the period 800-850 CE. Compared to the study performed by Solheim and Iversen (2019), similar results were found, as their study showed a demographic decrease from 400 CE to 800 CE, especially around 550 CE (429-30).

6.3.3 Abandonment in the Late Viking Age into the Early Middle Ages

From 925-950 CE a sharp increase in arboreal pollen takes place, indicating a reforestation of the area (appendix A.5). First *Betula* rapidly increases in the period 950-1100 CE (zone 6D), followed by an increase of *Pinus* between 1100 and 1500 CE (zone 7). Additionally, there is a sharp decrease in the number of charcoal particles in zone 6D and zone 7, which could indicate less human activity. Subsequently, in zone 6D, all anthropogenic indicators, such as *Artemisia*, *Chenopodiaceae*, *Urtica*, *Cannabis*, *Plantago major*, *Sordaria* and especially the cereal crops *Hordeum*, *Triticum*, *Avena* and *Secale* seem to cease (appendix A.5). The sudden disappearance of anthropogenic indicators after a period of rich agricultural activity, combined with a sudden increase in arboreal pollen, seems to suggest an abandonment of the area. Especially the rapid incline in pollen of *Betula*, a pioneer forest species, is likely to indicate natural

colonization of the landscape after abandonment of the land (Fischer et al. 2002, 17). The pollen assemblage does not only suggest a period with less cultivation, but also a period during which grazing activities seem to cease (appendix A.5).

Synchronous with the transition around 950 CE, a change in the lithology can be found. At a depth of approximately 86 cm the lithology (Figure 12) displays the occurrence of large, long grasses or roots, horizontally and vertically crossing the core. These grasses or roots could be a result of the environmental change displayed in the pollen record. However, grasses vertically crossing the peat sequence may also lead to a hiatus in the age-depth model and pollen record. Thus, the sharp 950 CE transition recognized in the pollen record could also be a reflection of a possible disturbance or hiatus in the peat sequence due to the grasses vertically crossing the peat sequence. In addition to that, it can be noted that the total sum of pollen shows a decrease around 950 CE (appendix A.1-4), supporting the hypothesis of a hiatus. However, the increase in arboreal pollen that proceeds after 950 CE, especially in pollen of *Pinus*, contradicts this hypothesis. After 950 CE the lithology of the peat sequence shows no possible indicators of disturbance. Thus, the increase in arboreal pollen proceeding after 950 CE provides evidence that a reforestation of the area did in fact occur.

As indicated by palynological studies of over 250 paleoenvironmental archives in southeastern Norway performed by H. I. Høeg (unpublished), an abandonment of the area around 950 CE, from the Late Viking Age into the Early Middle Ages has not been identified in other pollen assemblages before (personal communication Høeg 2021). Possible forcing factors for a sudden abandonment could be related to climate change or societal factors such as conflict. However, it must be noted that the sudden disappearance of anthropogenic indicators could also be caused by a disturbance or hiatus in the peat sequence

Amongst the burial ages at Bjørnstad burial site, only one burial was dated to this period, with a calibrated age of 772-986 CE. No burials dated younger than 986 CE were found. Although these results seem to correspond with the potential abandonment around 950 CE identified in the pollen record, it has to be taken into consideration that the absence of burials after 986 CE is likely due to the

emergence of Christianization. The results of the study by Solheim and Iversen showed a similar decrease in radiocarbon dates during the period of 1000-1500 CE. However, during their study, dates from medieval towns were not as systematically collected as dates from earlier periods (Solheim and Iversen 2019, 427). Christianization came to Norway around the 10th – 11th century, bringing fundamental changes for the societies including changes in burial practices (Solberg 2015, 275). Christian burial practices can be described as inhumation in a coffin. The coffins are buried in the ground orientated from east to west, where the head is positioned towards the west. An important change is the requirement that a burial should be located within a demarcated cemetery (Solberg 2015, 276). It became strictly forbidden to bury the dead in mounds or cairns, or next to a farm. Therefore, the decrease in radiocarbon dates after 986 CE could potentially be caused by the conversion to Christianity occurring around the time (Solberg 2015). However, in most places in Norway the conversion from heathen graves towards Christian graves occurred later, around the mid 11th century. Thus, it would be an early conversion compared to other regions in Norway.

The following table (Table 9) summarizes the main transitions as identified in the pollen record.

Table 9: Table summarizing the transitions analyzed in the pollen record of Haraldstadmyr bog.

Period	Age	Palynological zone	Cultural landscape	Description
<i>Early Bronze Age – Late Bronze Age</i>	1200 BCE – 800 BCE	3 and 4	Mixed farming	Decline in <i>Alnus</i> and incline in <i>Filipendula</i> suggesting the opening of pasture grounds.
<i>Late Bronze Age – Pre-Roman Iron Age</i>	800 BCE – 350 BCE	4	Reforestation of the area	Incline in arboreal pollen suggesting a reforestation of the area.
<i>Early Roman Iron Age – Late Roman Iron Age</i>	350 BCE – 300 CE	5	Pastoral farming	Clearance of the woodlands, grazing activities.
<i>Late Roman Iron Age</i>	300 CE – 450 CE	6A	Mixed farming	Indicators of both cultivation and grazing activities are presented
<i>Migration Period</i>	450 CE – 650 CE	6B	Potential abandonment of the area	Decline in cultivation activities, some grazing activities remain. Can be interpreted as a mid 6 th century abandonment.
	650 CE – 750 CE	6C	Pastoral farming	Indicators of grazing show an abundance.
	750 CE – 825 CE		Mixed farming	Abundance of all four cereal crops and indicators of grazing. Contemporary decline in arboreal pollen.
<i>Viking Period</i>	825 CE – 900 CE	6D	Pastoral farming	Incline in arboreal pollen; abrupt decrease in cereal crops. Indicators of grazing activities remain present.
	900 CE – 950 CE		Mixed farming	High cultivational activity, sharp decrease in arboreal pollen until 925 CE.
	925 CE		Reforestation of the area	Sharp increase in arboreal pollen.
	950 CE	Potential abandonment of the area	Abrupt disappearance of anthropogenic indicators, combined with an increase in arboreal pollen.	

6.4 Forcing factors of transitions in the pollen record

The changes found in the cultural landscape (Table 9) could potentially be a result of climate change. The decrease in cultivation crops seen in the mid 6th century has been found in multiple pollen records in Northern-Europe (Bajard et al. unpublished; Høeg unpublished; Iversen 2013,1). A cold period that is known to have occurred in the Northern hemisphere from 536 CE to approximately 660 CE is often referred to as the Late Antique Little Ice Age (Büntgen et al. 2016). This cold period was onset by a volcanic double event (Toohey et al. 2016) and prolonged by a series of large eruptions in 536 CE, 540 CE, 547 CE until 660 CE (van Dijk et al. 2021). As a result, a significant drop in temperature of 4-5 degrees Celsius in Scandinavia, combined with a decrease in precipitation (van Dijk et al. 2021) led to a period of crop failure, famine and farm abandonment (Iversen 2013, 3; Toohey et al. 2016). The decrease in agricultural intensity recognized in the pollen record of Haraldstadmyr bog from 450-650 CE is contemporary with the Late Antique Little Ice Age. As a result, this colder climatic period could potentially have been the forcing factor of the decrease in crop cultivation recognized in the pollen assemblage of Haraldstadmyr bog.

Other factors related to climate that could impact changes in the pollen record through time include precipitation. Periods with increased precipitation alternated by drier periods can cause changes in the pollen record. Interpretations about the past precipitation levels can to a certain degree be derived from the lithology of the core. The occurrence of tree roots in the peat sequence can indicate a disturbance of the surface of the bog by trees during a drier climatic period (Lowe and Walker 2015, 161). In addition to that, transitions in the lithology from the dark well-humified peat to light-coloured less humified Sphagnum peat can mark changes in precipitation (Lowe and Walker 2015, 162). The upper part of Haraldstadmyr peat sequence showed various transitions from darker Sphagnum peat to lighter Sphagnum peat (0-60 cm), which could signal variations in precipitation from 1150 to 1850 CE (palynological zone 7). Towards the basal part of the peat sequence, from 232 to 242 cm a layer of tree roots was identified, which could represent a drier climatic period. These depths correlate with 2450 BCE to 2200 BCE (palynological zone 2). However, so far, no clear lithological

changes signaling precipitation change could be correlated to the main transitions that were identified in the pollen record.

Apart from forcing factors related to climate, factors related to societal change should also be taken into consideration. From 541-750 CE the Justinian Plague, spread through Europe and highly impacted the population rate (Little 2007). In combination with a contemporary occurrence of the cold period, changes in the organization of society took place. Iversen (2013) showed that farms were often divided into smaller production units and marginal areas were often completely abandoned (Iversen 2013). The impact of the Justinian Plague on the population rate in Europe is reflected in the decrease in radiocarbon ages at Bjørnstad burial site, which was identified from 600-800 CE. Studies have shown that the Justinian Plague possibly amplified as a result of the global cooling driven by volcanic eruptions in the same period in time (Kausrud et al 2010).

In addition to the Justinian Plague, recent studies discovered the presence of the smallpox virus in human remains in Norway in the 7th century (Mühlemann et al. 2020). A combination of these factors could potentially have caused the decrease in anthropogenic indicators in the pollen record of Haraldstadmyr bog during the mid 6th century, as well as the decrease in radiocarbon dates seen at Bjørnstad burial site.

The potential abandonment recognized in the pollen record around 950 CE, however, has not been found in previous studies. From 800 CE onwards, a climatic warming is known to have occurred in Scandinavia, which caused agricultural practices in the majority of Scandinavia to increase and develop (Bajard et al. unpublished). Since the sudden decline in agricultural intensity recognized in the pollen record of Haraldstadmyr bog occurred during a relatively warm period, it is more likely that the forcing factors of this potential abandonment were related to societal change. In addition, there is a lack of similar indicators of abandonment in other pollen records from Southeastern Norway. Therefore, it is important to note that an abandonment could have occurred solely on a local scale. Other causes for the sudden disappearance of anthropogenic indicators in the pollen record could be related to a disturbance in the peat sequence as noted in chapter 6.3.3.

6.5 Reliability and limitations of the study

The current study contained several limitations affecting the reliability of the findings. First of all, the pollen analysis was performed at a higher resolution between depths of 80 and 130 cm when compared to the rest of the peat sequence. The variation in sampling resolution in the peat archive could result in a biased analysis of the pollen record. From 80-130 cm samples were taken for each centimeter in this section, compared to samples for each 5 or 10 centimeters in the rest of the peat sequence. Thus, transitions in the pollen record can be seen in great detail from 80 to 130 cm, whereas plausible transitions in the rest of the pollen record might remain invisible and thus unacknowledged. In addition, there is a higher chance of anthropogenic indicators being identified in the section that is of high resolution, as compared to the section below and above it.

Additional limitations include the interpretation of pollen data: the production, dispersal, deposition and preservation of the pollen differ for each type of plant, as explained in chapter 1.8. These differences can cause an over-representation of certain types of plants, as well as an under-representation of other types of plants (Lowe and Walker 2015, 169-172).

The age-depth model in this study was generated utilizing Bayesian-based modelling. This model assumes the accumulation rate of the peat bog between the different dated levels to be constant. Whereas in general the accumulation rate in sphagnum peat can be assumed to be constant due to the constancy of growth and die-back of *Sphagnum* (Neef and Cappers 2012, 148), irregularities in the sedimentation rate can occur due to fluctuations in climatic conditions or due to the impact of humans, such as the cultivation of crops or the harvesting of peat for fuel purposes (Neef and Cappers 2012, 148). The latter can cause a stagnation in the development of the peat. Thus, it has to be taken into consideration that the assumption of linearity can cause errors in the age-depth model (Neef and Cappers 2012, 148). Furthermore, due to the use of radiocarbon dates for the age-depth model, the chronology provided in this study contains a standard deviation. Thus, even though the pattern of transitions throughout the pollen record remains the same, the absolute dating of these transitions contains a standard deviation.

The age-depth model used in this study is most reliable at the upper part of the peat sequence (0-123.5 cm) as a sufficient number of radiocarbon samples were dated in this section. From the basal part of the peat sequence (123.5-282 cm) only one radiocarbon date was available, at a depth of 267.5 cm. This radiocarbon date originates from a different core, as explained in chapter 3.2, which causes a high uncertainty. In addition, the age-depth model merely estimates the ages of the sediment between the dated levels of 123,5 cm and 267,5 cm, proposing a wide range of plausible ages. Therefore, the age-depth model should be considered unreliable from 123.5 to 282 cm. As a consequence, the current study focused on the more recent part of the age-depth model, from the Iron Age to the Middle Ages. As described in appendix C, new samples were taken and sent out for radiocarbon dating in order to improve the age-depth model. Unfortunately, these samples were not analysed in time to be included in the current study.

Radiocarbon dating involves other potential risks that can cause errors, such as the reservoir effect. The reservoir effect is the effect during which a sample obtains its carbon from another reservoir than the atmosphere. Usually, the carbon obtained in the sample has a lower ^{14}C level than the atmosphere, resulting in a measured age that is too old (Philippsen 2013, 1). However, a study conducted by Blaauw et al. (2004) found the reservoir effect to be absent in their samples extracted from a peat bog core. As a result, the risk of selecting aquatic plants influenced by the reservoir effect seems to be relatively low.

7. Conclusion

7.1 Summary and conclusions

This thesis attempted to provide a high-resolution chronology of agricultural practices in southeastern Norway from the Early Iron Age to the Middle Ages, as well as to reconstruct the paleoenvironment of the area through time. Both the paleoenvironment and the cultural landscape of the area of Haraldstadmyr in Southeastern Norway were studied by analyzing a pollen data set of exceptionally high resolution, to answer to following research questions:

Which transitions can be found within the pollen record?

How has the local and regional vegetation of the peat bog developed through time?

How has the cultural landscape developed from the Early Iron Age to the Middle Ages?

Which variations in agricultural activities and farming intensity can be interpreted from the pollen record from the Early Iron Age to the Middle Ages?

How do the findings from the palynology compare to the dated burials at Bjørnstad burial site as well as other archaeological finds in the area?

Which forcing factors could potentially have caused the transitions seen in the pollen record?

Table 9 summarizes the transitions recognized in the pollen record. At a local scale, the peat bog developed from the wet environment of a lake, into a fen and gradually into the terrestrial environment of a raised bog. At a regional scale, a transition was recognized around 1200 BCE, where a decline in arboreal pollen such as *Alnus* was followed by an increase in *Filipendula* suggesting a deforestation and the opening up of pasture grounds. From 1200 – 800 BCE, a period of farming and cultivation was suggested due to the appearance of several anthropogenic indicators. Subsequently, from 800 – 350 BCE, a period of reforestation took place, followed by a clearing of the woodland around 350 BCE.

The pollen record shows the presence of agricultural practices in the area from 350 until 950 CE, although the intensity and the type of agricultural practices

varied throughout this period. This period was studied in further detail in order to reconstruct the cultural landscape from the Early Iron Age to the Middle Ages.

The main findings show three important transitions in the cultural landscape (Table 9). The first transition describes the onset of active pastoral farming activities around 350 BCE, after a period of less intensive farming and reforestation from 800 BCE to 350 BCE. From 300 CE onwards, more cultivation occurs next to the grazing activities, presenting a period of mixed farming up to 450 CE. As a second transition, a decline in cultivation activities was found during the mid 6th century, lasting for approximately 200 years, from 450 to 650 CE. The subsequent period from 650-950 CE shows a rich period in agricultural activities.

Due to the high-resolution nature of the pollen data, four phases of farming could be distinguished during this period. An alternation was found between periods of mixed farming and periods of grazing, as represented in Table 9. Around 925 CE a sharp increase in arboreal pollen announces a reforestation of the area, followed by a sudden disappearance of anthropogenic indicators around 950 CE. In combination with the increase in arboreal pollen the disappearance of anthropogenic indicators suggests an abandonment of the farming area. A similar abandonment of the area around 950 CE has not been previously recognized in southeastern Norway.

Archaeological dates from a graveyard site named Bjørnstad, located next to Haraldstadmyr, were studied in comparison to the pollen record in order to find a correlation between farming activity recognized in the pollen record and archaeological evidence of habitation of the area. The burial dates indicate continuous habitation in the area from the Pre-roman Age into the Viking period, from approximately 172 BCE to 986 CE, where most burial dates were dated to the Roman Iron Age, up until 400 CE. Subsequently, a decrease in the number of burial dates was found, suggesting a similar mid 6th century abandonment as recognized in the pollen record. Although the lack of dates from 986 CE seem to correspond with the 950 CE abandonment recognized in the pollen record, the

absence of the burial dates is most likely caused by to the emergence of Christianization.

Plausible forcing factors of the transitions found within the pollen record were discussed. Possible forcing factors for the mid 6th century abandonment seen in the pollen record include climate cooling as well as the spread of the Justinian plague. However, forcing factors of the mid 10th century abandonment remain unidentified. Climate change is unlikely to have served as a forcing factor for the 950 CE abandonment, as this period in time is known to have been a relatively warm period. In addition, the abandonment has not been recognized in other pollen records in southeastern Norway (personal communication, Høeg 2021). Therefore, the abandonment is more likely to have been an effect of societal change or conflict.

7.2 Further research

In order to confirm the main findings about the past regional vegetation and cultural landscape in southeastern Norway further research is needed. The 950 CE abandonment of the area is a new finding that has not been previously reported. However, few palynological studies have been performed with a similar resolution as the current study. Therefore, more pollen records in the area of a similar resolution need to be analyzed and compared in order to confirm an abandonment of the area around 950 CE. Additionally, the standard deviation of the radiocarbon dates used for the age-depth model in the present study causes an uncertainty when it comes to the chronology of the pollen record of Haraldstadmyr bog. Absolute dating methodologies, such as tephrochronology, are required in order to improve the age-depth model of the peat sequence.

Furthermore, additional research is needed in order to establish the forcing factors of the transitions recognized in the cultural landscape and regional vegetation of Haraldstadmyr bog area. Research devoted to climate variability of the area could reveal a plausible causal relation between the transitions in the pollen record and climate change, such as the adaptation of agricultural practices to climate variability as analyzed by Bajard et al. (unpublished) in a lake in southeastern Norway. In addition, more literary review and historical analysis is required to search for societal changes and conflicts in the area as a plausible cause of transitions in the pollen record.

Abstract

Human activities have impacted the natural landscape and vegetation from the emergence of agriculture onwards. Subsequent traces of anthropogenic activities are documented and preserved in paleoenvironmental archives, such as peat or lake sequences. The current study utilizes a high-resolution pollen dataset retrieved from a peat sequence in combination with archaeological data from the area to reconstruct the paleoenvironment and cultural landscape of the area of Haraldstadmyr bog in Southeastern Norway. An in-depth analysis of agricultural activities was performed focusing on the period of the Early Iron Age to the Medieval Period. Utilizing radiocarbon dating, a chronology of farming activities was provided. Archaeological burial dates from a local burial site located were used in comparison with the pollen data to interpret habitational patterns of the local area. As a result, periods of intensive farming as well as periods of abandonment were identified. In addition, periods of pastoral farming were distinguished from periods of mixed farming. The forcing factors of the changes seen in farming strategies and agricultural intensity are likely related to climate changes as well as societal changes in the area. In this study, a new finding is proposed, indicating an abandonment of the area around 950 CE. An abandonment of the agricultural area in Southeastern Norway in the mid 10th century has not been previously discovered nor studied. Further in-depth studies are needed in order to confirm this finding, as well as to identify the forcing factors of the abandonment.

Bibliography

- Bajard, M., Ballo, E., Høeg, H. I., Bakke, J., Støren, E., Loftsgarden, K., Iversen, F., Hagopian, W., Jahren, A. H., Svensen, H. H., and K. Krüger, unpublished. Climate variability controlled the pre-Viking society development during the Late Antiquity in Southeastern Norway.
- Bakels, C., 2020. Pollen and Archaeology, A. G. Henry (eds), in *Handbook for the Analysis of Micro-Particles in Archaeological samples*. Cham: Springer Nature Switzerland (Interdisciplinary Contributions to Archaeology), 203-224.
- Behre, K., 1981. Anthropogenic Indicators in Pollen Diagrams. *Pollen et Spores* 23, 225–245.
- Bell, M.A. and J. M. Blais, 2021. Paleolimnology in support of archeology: a review of past investigations and a proposed framework for future study design. *Journal of Paleolimnology* 65(1), 1–32.
- Berger, S., G. Gebauer, C. Blodau and K. H. Knorr, 2017. Peatlands in a eutrophic world – Assessing the state of a poor fen-bog transition in southern Ontario, Canada, after long term nutrient input and altered hydrological conditions. *Soil Biology and Biochemistry* 114, 131–44.
- Bjune, A. E., 2005. Holocene vegetation history and tree-line changes on a north south transect crossing major climate gradients in southern Norway evidence from pollen and plant macrofossils in lake sediments. *Review of Palaeobotany and Palynology* 133(3–4), 249–275.
- Blaauw, M., van der Plicht, J. and B. van Geel, 2004. Radiocarbon dating of bulk peat samples from raised bogs: non-existence of a previously reported ‘reservoir effect’? *Quaternary Science Reviews* 23(14–15), 1537–1542.
- Blaauw, M. and J. A. Christen, 2011. Flexible paleoclimate age-depth models using an autoregressive gamma process. *Bayesian Anal* 6, 457–474.
- Büntgen, U., V.S. Myglan, F.C. Ljungqvist, M. McCormick, N. Di Cosmo, M. Sigl, J. Jungclaus, S. Wagner, P.J. Krusic, J. Esper, J.O. Kaplan, M.A.C. de Vaan, J. Luterbacher, L. Wacker, W. Tegel and A.V. Kirilyanov, 2016. Cooling and societal change during the Late Antique Little Ice Age from 536 to around 660 AD. *Nature Geoscience* 9(3), 231–36.

- Brandal, M. K. and E. Heder, 1991. Stratigraphy and sedimentation of a terminal moraine deposited in a marine environment- two examples from the Ra ridge in Østfold, southeast Norway. *Norsk Geologisk Tidsskrift* 71, 3-14.
- Bronk Ramsey, C., 2009. Bayesian analysis of radiocarbon dates. *Radiocarbon* 51(1), 337–360.
- Danielsen, A. 1970. *Pollen-analytical Late Quaternary studies in the Ra district of Østfold, southeast Norway*. Oslo: Norwegian Universities Press Bergen.
- Felde, V.A., S.M. Peglar, A.E. Bjune, J.-A. Grytnes and H.J.B. Birks, 2014. The relationship between vegetation composition, vegetation zones and modern pollen assemblages in Setesdal, southern Norway. *The Holocene* 24(8), 985–1001.
- Fischer, A., Lindner, M., Abs, C., and P. Lasch, 2002. Vegetation dynamics in central European forest ecosystems (near-natural as well as managed) after storm events. *Folia Geobotanica*, 37(1), 17-32.
- Fjellstad, W.J. & W.E. Dramstad, 1999. Patterns of change in two contrasting Norwegian agricultural landscapes. *Landscape and Urban Planning* 45 (1999), 177-191.
- Frew, C.R., 2014. Coring Methods. *Geomorphological Techniques* 4 (1.1), 1-10.
- Fægri, K. and J. Iversen, 1989. *Textbook of pollen analysis*. Chichester: John Wiley & sons.
- Gaillard, M. J., 2013. POLLEN METHODS AND STUDIES. Archaeological Applications. *Encyclopedia of Quaternary Science*, 880–904.
- Goring, S., Dawson, A., Simpson, G. L., Ram, K., Graham, R. W., Grimm, E. C., and J. W. Williams, 2015. neotoma: A Programmatic Interface to the Neotoma Paleoecological Database. *Open Quaternary* 1(1), Art. 2. DOI: 10.5334/oq.ab
- Høeg, H. I., unpublished. POLLENANALYTISKE UNDERSØKELSER AV HARALDSTADMYR, BJØRNSTAD, SARPSBORG, ØSTFOLD., 1-7.
- Hjelle, K.L., T. Solem, L.S. Halvorsen, and L.I. Åstveit, 2012. Human impact and landscape utilization from the Mesolithic to medieval time traced by high spatial resolution pollen analysis and numerical methods. *Journal of Archaeological Science* 39(5), 1368–1379.
- Iversen, F., 2013. Big bang, lordship or inheritance? Changes in the settlement structure on the threshold of the Merovingian Period, South-Eastern

- Norway. *Hierarchies in Rural Settlements* 9, 341–358.
- Iversen, F., 2017. Prosjektplan for Bjørnstadveien 50, id81303 (gravfelt og bosetningsspor). *Universitetet i Oslo, Kulturhistorisk Museum, Arkeologisk seksjon*.
- Iversen, F., 2018. Prosjektbeskrivelse av arkeologisk undersøkelse av id 115688 Haraldstadmyra (offersted). *Universitetet i Oslo, Kulturhistorisk Museum, Arkeologisk seksjon*.
- Juggins, S., 2020. rioja: Analysis of Quaternary Science Data. R package version 0.9-26, <https://cran.r-project.org/package=rioja>.
- Kausrud, K. L., Begon, M., Ari, T. B., Viljugrein, H., Esper, J., Buntgen, U., Leirs, H., Junge, C., Yang, B., Yang, M., Xu, L. and N. C. Stenseth, 2010. Modeling the epidemiological history of plague in Central Asia: Palaeoclimatic forcing on a disease system over the past millennium. *BMC Biology* 8(1), 112.
- Kruusamägi, I. 2015. Avaste Fen, Estonia. Sedges dominate the landscape, woody shrubs and trees are sparse.
- Larsen, J., Bjune, A. E. and A. de la Riva Caballero, 2006. Holocene Environmental and Climate History of Trettetjørn, a Low-alpine Lake in Western Norway, Based on Subfossil Pollen, Diatoms, Oribatid Mites, and Plant Macrofossils. *Arctic, Antarctic, and Alpine Research* 38 (4), 571-583. [https://doi.org/10.1657/1523-0430\(2006\)38\[571:HEACHO\]2.0.CO;2](https://doi.org/10.1657/1523-0430(2006)38[571:HEACHO]2.0.CO;2)
- Li, Y., L. Zhou and H. Cui, 2008. Pollen indicators of human activity. *Science Bulletin* 53(9), 1281–93.
- Lowe, J. J., and M. Walker, 2015. *Reconstructing quaternary environments*. New York: Routledge/Taylor & Francis Group.
- Mehl, I K., and K. L. Hjelle, 2015. From pollen percentage to regional vegetation cover — A new insight into cultural landscape development in western Norway. *Review of Palaeobotany and Palynology* 217, 45–60.
- Mickel, J. T., Gifford, E. M., Wagner, Warren H., Yatskievych, G. and F. W. Walker, 2020. "Fern". *Encyclopedia Britannica*, accessed 7 May 2021.
- Mühlemann, B, Vinner, L, Margaryan, A, Wilhelmson, H, de la Fuente Castro, C, Allentoft, ME, de Barros Damgaard, P, Hansen, AJ, Holtmark Nielsen, S, Strand, LM, Bill, J, Buzhilova, A, Pushkina, T, Falys, C, Khartanovich, V, Moiseyev, V, Jørkov, MLS, Østergaard Sørensen, P, Magnusson, Y,

- Gustin, I, Schroeder, H, Sutter, G, Smith, GL, Drostén, C, Fouchier, RAM, Smith, DJ, Willerslev, E, Jones, TC and M. Sikora, 2020. Diverse variola virus (smallpox) strains were widespread in northern Europe in the Viking Age. *Science* 369 (6502), <https://doi.org/10.1126/science.aaw8977>
- Neef, R., and R. T. J. Cappers, 2012. *Handbook of Plant Palaeoecology*. Groningen Archaeological Studies 19. Eelde: Barkhuis.
- Nichols, G. 2009. *Sedimentology and stratigraphy*. Chichester: Wiley-Blackwell.
- O'Reilly, B. C., S.A. Finkelstein and J. Bunbury, 2014. Pollen-Derived Paleovegetation Reconstruction and Long-Term Carbon Accumulation at a Fen Site in the Attawapiskat River Watershed, Hudson Bay Lowlands, Canada. *Arctic, Antarctic, and Alpine Research* 46(1), 6–18.
- Overland, A., and K. L. Hjelle, 2009. From forest to open pastures and fields: cultural landscape development in western Norway inferred from two pollen records representing different spatial scales of vegetation. *Vegetation History and Archaeobotany* 18(6), 459–476.
- Philippsen, B., 2013. The freshwater reservoir effect in radiocarbon dating. *Heritage Science* 1(24), 1-19.
- Prøsch-Danielsen, L., 1993. Prehistoric agriculture revealed by pollen analysis, plough-marks and sediment studies at Sola, south-western Norway. *Vegetation History and Archaeobotany* 2(4), 233-244.
- Reimer, P. J, Austin, W. E. N., Bard, E., Bayliss, A., Blackwell, P. G., Ramsey, C. B., Butzin, M., Cheng, H., Edwards, R. L., Friedrich, M., Grootes, P. M., Guilderson, T. P., Hajdas, I., Heaton, T. J., Hogg, A. G., Hughen, A. K., Kromer, B., Manning, S. W., Muscheler, R., Palmer, J. G., Pearson, C., van der Plicht, J., Reimer, R. W., Richards, D. A., Scott, E. M., Southon, J. R., Turney, C. S. M., Wacker, L., Adolphi, F., Büntgen, U., Capano, C., M Fahrni, M. F., Fogtmann-Schulz, A., Friedrich, R., Köhler, P., Kudsk, S., Miyake, F., Olsen, J., Reinig, F., Sakamoto, M., Sookdeo, A. and S. Talamo., 2020. THE INTCAL20 NORTHERN HEMISPHERE RADIOCARBON AGE CALIBRATION CURVE (0–55 CAL kBP). *Radiocarbon*, 1–33. DOI:10.1017/RDC.2020.41.
- Solberg, B., 2000. *Jernalderen i Norge. 500 før Kristus til 1030 etter Kristus*. Oslo: Cappelen Akademisk.
- Solheim, S. and Iversen, F., 2019. The mid-6th century crises and their impacts on

- human activity and settlements in south-eastern Norway, in: Niall Brady & Claudia Theune (eds), *Ruralia XII: Settlement change across Medieval Europe; old paradigms and new vistas*. Leiden: Sidestone Press, 423–433.
- Stivirins, N., I. O., and M. Gałka, 2017. Drivers of peat accumulation rate in a raised bog: impact of drainage, climate, and local vegetation composition. *Mires and Peat* (19), 1–19.
- Toohey, M., Krüger, K., Sigl, M., Stordal, F. and H. Svensen., 2016. Climatic and societal impacts of a volcanic double event at the dawn of the Middle Ages. *Climatic Change* 136(3–4), 401–412.
- Van Dijk, E., J. Jungclauss, S. Lorenz, C. Timmreck and K. Krüger, 2021. Was there a volcanic induced long lasting cooling over the Northern Hemisphere in the mid 6th–7th century? DOI:10.5194/cp-2021-49.
- Van Geel, B., J. Buurman, O. Brinkkemper, J. Schelvis, A. Aptroot, G. Van Reenen & T. Hakbijl, 2003. Environmental reconstruction of a Roman Period settlement site in Uitgeest (The Netherlands), with special reference to coprophilous fungi. *Journal of Archaeological Science* 30(7), 873–83.
- Wickham, H., 2016. *ggplot2: Elegant Graphics for Data Analysis*. New York (NY): Springer.
- Wickham et al., 2019. Welcome to the tidyverse. *Journal of Open Source Software*, 4(43), 1686. <https://doi.org/10.21105/joss.01686>
- www.kartverket.no, accessed on 5 April 2021.
- www.raisedbogs.ie, accessed on 2 March 2021

8. Figures, tables and appendices

8.1 Figures

Figure 1: Sampling for radiocarbon dating, Haraldstadmyr peat sequence, 2021.	1
Figure 2: Map of Norway showing the location of the study site situated in Østfold, Southeastern Norway indicated by the red dot (kartverket.no).	11
Figure 3: An aerial photograph depicting the current vegetation of Haraldstadmyr Bog, Østfold, Southeastern Norway (kartverket.no).	12
Figure 4: Elevation map depicting Haraldstadmyr bog, Østfold, Southeastern Norway (høydedata.no).	13
Figure 5: Location of the excavation site at Haraldstadmyr bog. The excavated area is depicted in green (Iversen 2018).	14
Figure 6: Haraldstadmyr excavation, November 2020.	14
Figure 7: The Ra-ridge running through both Østfold and Vestfold county, with the red dot indicating the location of Haraldstadmyr bog (Brandal & Heder 1991, 3).	15
Figure 8: A schematic depiction of the hydroseral succession and the development from limnic peats in lakes to terrestrial peats under oligotrophic conditions (Lowe and Walker 2015, 154).	20
Figure 9: Schematic representation of the development of a lake to a raised bog (Lowe and Walker 2015, 154).	21
Figure 10: H.I. Høeg sampling the peat sequence at Haraldstadmyr bog, Southeastern Norway (Iversen 2018).	28
Figure 11: The sampling location of the peat sequence at Haraldstadmyr bog, Southeastern Norway (Iversen 2018).	28
Figure 12: The lithology of the peat sequence of Haraldstadmyr bog.	35
Figure 13: Age-depth model of Haraldstadmyr bog peat sequence showing the calibrated ages according to depth.	38
Figure 14: Plot showing the distribution of the calibrated radiocarbon dates from the structures at Bjørnstad burial site according to time, where the probability distribution for each date is displayed in grey.	50
Figure 15: Plot displaying the distribution of the calibrated radiocarbon dates from the burials located at Bjørnstad burial site according to time, where the probability distribution for each date is depicted in grey.	52
Figure 16: Plot displaying the distribution of the calibrated radiocarbon dates from the burials located at Bjørnstad burial site according to time, where the probability distribution for each date is depicted in grey.	53
Figure 17: Graph showing the distribution of the number of dated graves found at Bjørnstad burial site categorized into different periods in time, using an interval of 200 years.	55
Figure 18: Picture showing the local vegetation of a fen, such as small trees of the species Salix and Alder (Kruusamägi 2015).	57

Figure 19: Picture showing the local vegetation commonly found at raised bogs, such as the heather types *Ericales*, *Empetrum* and *Calluna* (<http://raisedbogs.ie/>). 58

Tables

Table 1: Distribution of vegetation types accounted for in Rakkestad and Hjartdal municipalities during the 1950s and 1990s (Fjellstad and Dramstad 1999).	17
Table 2: Table showing an estimate of pollen production amongst common plant species in Europe (Lowe and Walker 2015, 191).	24
Table 3: The depths in cm for each core	34
Table 4: Table showing the uncalibrated (after Høeg 2018) and calibrated radiocarbon ages for each sample from Haraldstadmyr peat archive .	37
Table 5: Different zones as defined in the pollen diagrams, with their according ages and depths.	39
Table 6: Table showing the calibrated dates of different structures from Bjørnstad burial site (source?).	48
Table 7: Table showing the calibrated radiocarbon dates from the burials located at Bjørnstad burial site (source).	51
Table 8: Table showing the number of dated graves found at Bjørnstad burial site for each period in time, ranging from the Pre-roman Iron Age to the Viking period, using an interval of 200 years.	54
Table 9: Table summarizing the transitions analyzed in the pollen record of Haraldstadmyr bog.	65
Table 10: Samples taken for radiocarbon dating in February 2021	92

8.4 Appendices

Appendix A: Percentage pollen diagrams of Haraldstadmyr peat sequence.	83
Appendix A.1: Part one of the percentage pollen diagram showing the entire pollen record of Haraldstadmyr peat sequence according to cal. age (BCE/CE), subdivided into 9 palynological zones indicated to the right. Pollen types that were multiplied by 10 or 20 are indicated with (x10) or (x20) in the title for each pollen type. The lithology of the peat sequence and their according depths (cm) are indicated to the left of the diagram. The total pollen sum (ΣP) for each depth is indicated to the right, shown multiplied by 0.1. Percentages of pollen, spores and non- pollen palynomorphs outside the pollen sum (X) are based on ($\Sigma P+X$). The shaded curves show x20 exaggerations.	83
Appendix A.2: Part two of the percentage pollen diagram showing the entire pollen record of Haraldstadmyr peat sequence according to cal. age (BCE/CE), subdivided into 9 palynological zones indicated to the right. Pollen types that were multiplied by 10 or 20 are indicated with (x10) or (x20) in the title for each pollen type. The lithology of the peat sequence and their according depths (cm) are indicated to the left of the diagram. The total pollen sum (ΣP) for each depth is indicated to the right, shown multiplied by 0.1. Percentages of pollen, spores and non- pollen palynomorphs outside the pollen sum (X) are based on ($\Sigma P+X$). The shaded curves show x20 exaggerations.	84

Appendix A.3: Part three of the percentage pollen diagram showing the entire pollen record of Haraldstadmyr peat sequence according to cal. age (BCE/CE), subdivided into 9 palynological zones indicated to the right. Pollen types that were multiplied by 10 or 20 are indicated with (x10) or (x20) in the title for each pollen type. The lithology of the peat sequence and their according depths (cm) are indicated to the left of the diagram. The total pollen sum (ΣP) for each depth is indicated to the right, shown multiplied by 0.1. Percentages of pollen, spores and non- pollen palynomorphs outside the pollen sum (X) are based on ($\Sigma P+X$). The shaded curves show x20 exaggerations.

.....85

Appendix A.4: Percentage pollen diagram showing the main pollen type categories of the entire pollen record of Haraldstadmyr peat sequence according to cal. age (BCE/CE), subdivided into 9 palynological zones indicated to the right. The lithology of the peat sequence and their according depths (cm) are indicated to the left of the diagram. The total pollen sum (ΣP) for each depth is indicated to the right, shown multiplied by 0.1.

.....86

Appendix A.5: Selective percentage pollen diagram showing a selection of trees and shrubs, and the anthropogenic indicators of the pollen record of Haraldstadmyr peat sequence according to cal. age (BCE/CE), from 450 BCE to 1500 CE. Pollen types that were multiplied by 10 or 20 are indicated with (x10) or (x20) in the title for each pollen type. The lithology of the peat sequence and their according depths are indicated to the left of the diagram. The total pollen sum (ΣP) for each depth is indicated to the right, shown multiplied by 0.1. Percentages of pollen, spores and non- pollen palynomorphs outside the pollen sum (X) are based on ($\Sigma P+X$). The shaded curves show x20 exaggerations.

.....87

Appendix B: The uncalibrated radiocarbon dates from Bjørnstad burial site (Iversen 2018).

.....88

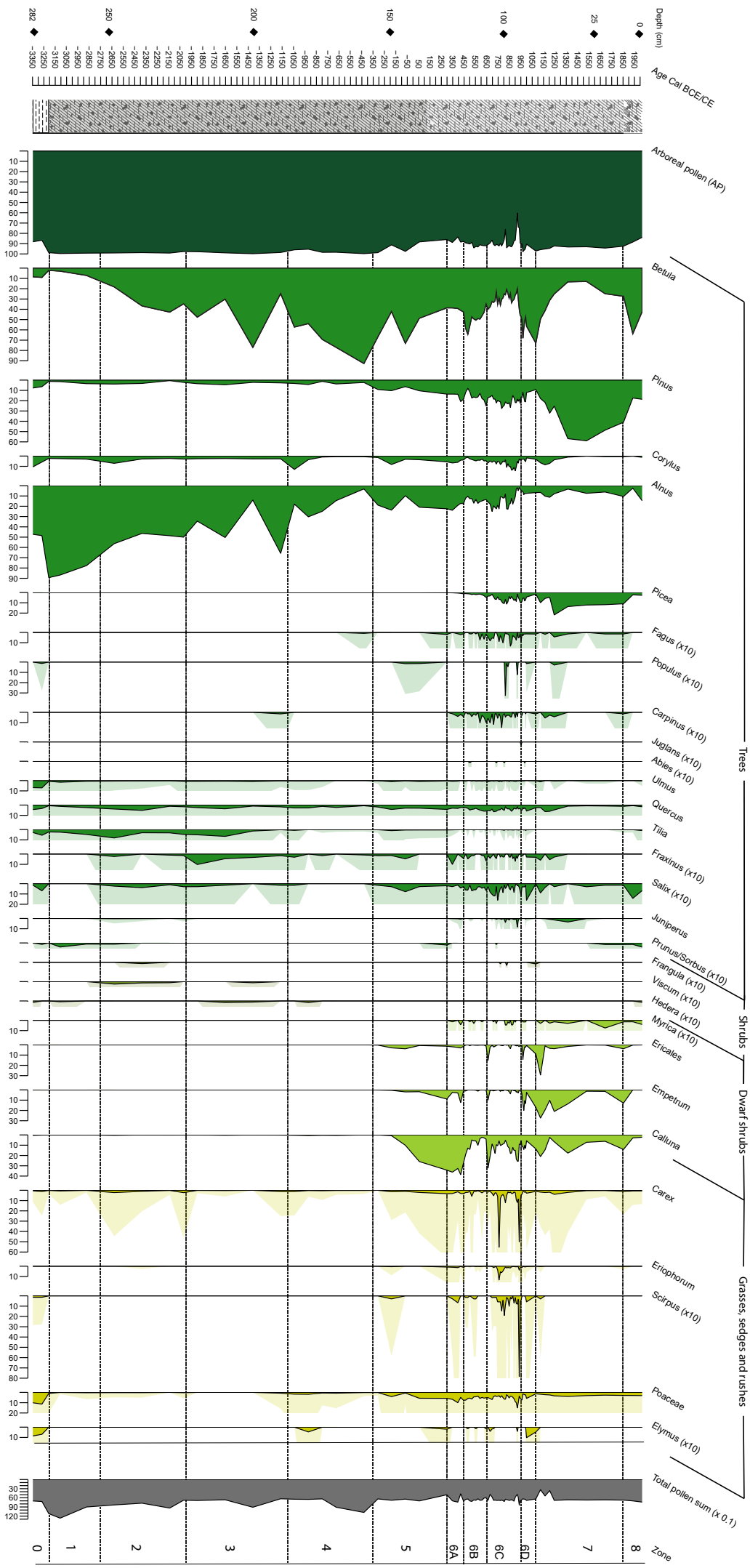
Appendix C: New ¹⁴C radiocarbon dating in 2021

.....92

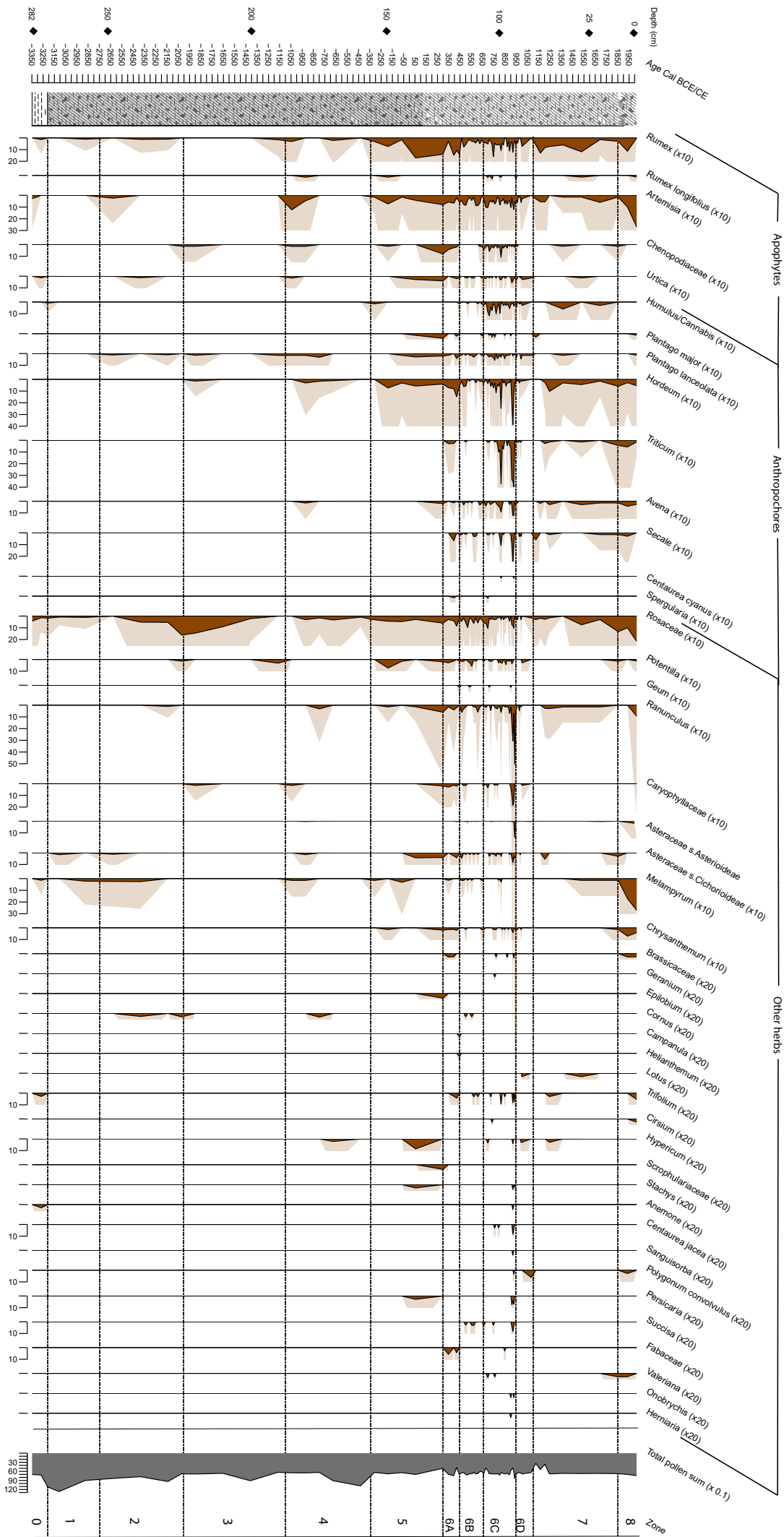
Appendix D: The script used for plotting the pollen diagrams in 'R'.

.....93

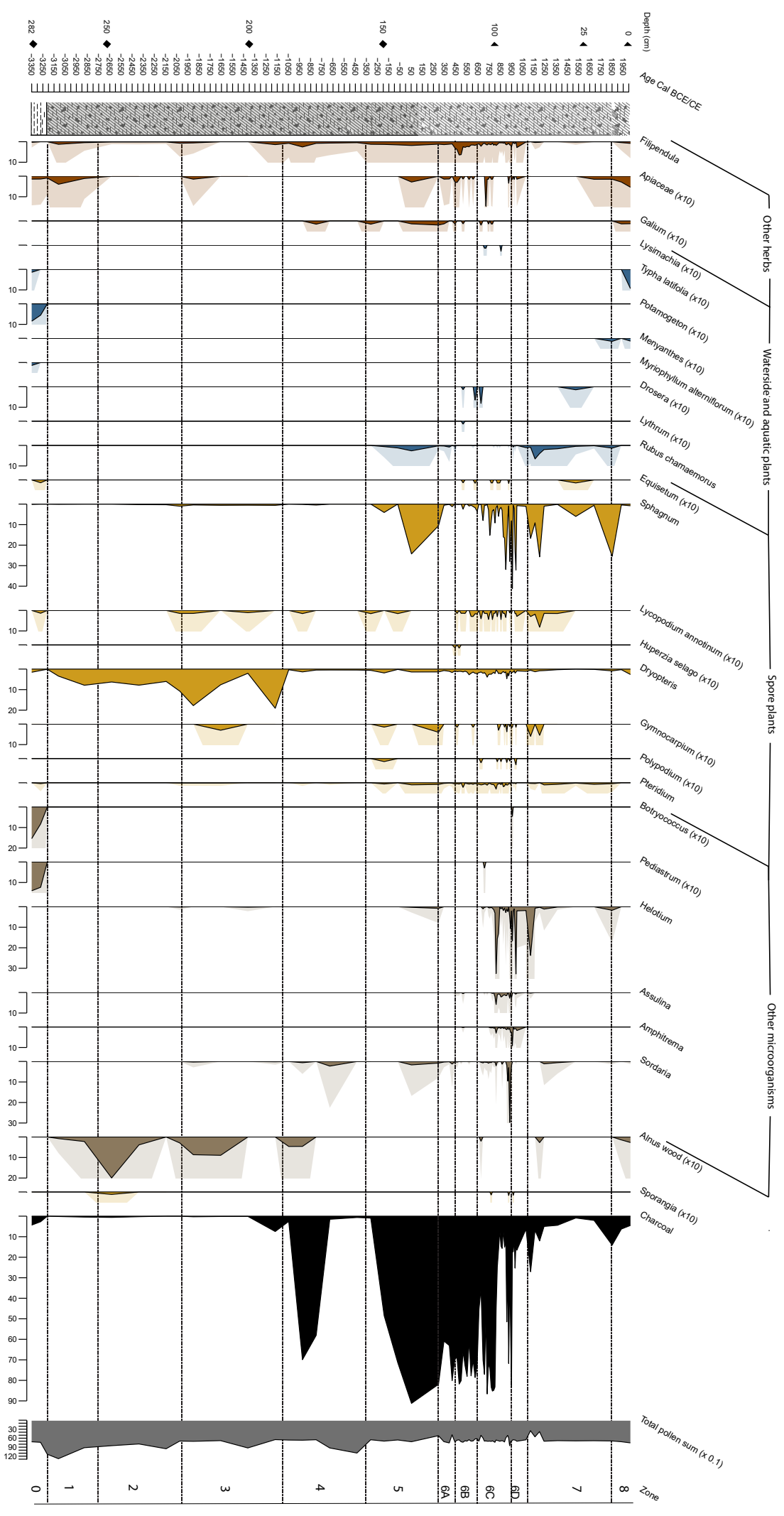
Appendix A.1: Part one of the percentage pollen diagram showing the entire pollen record of Haraldstadmyr peat sequence (see page 82 for the complete figure description).



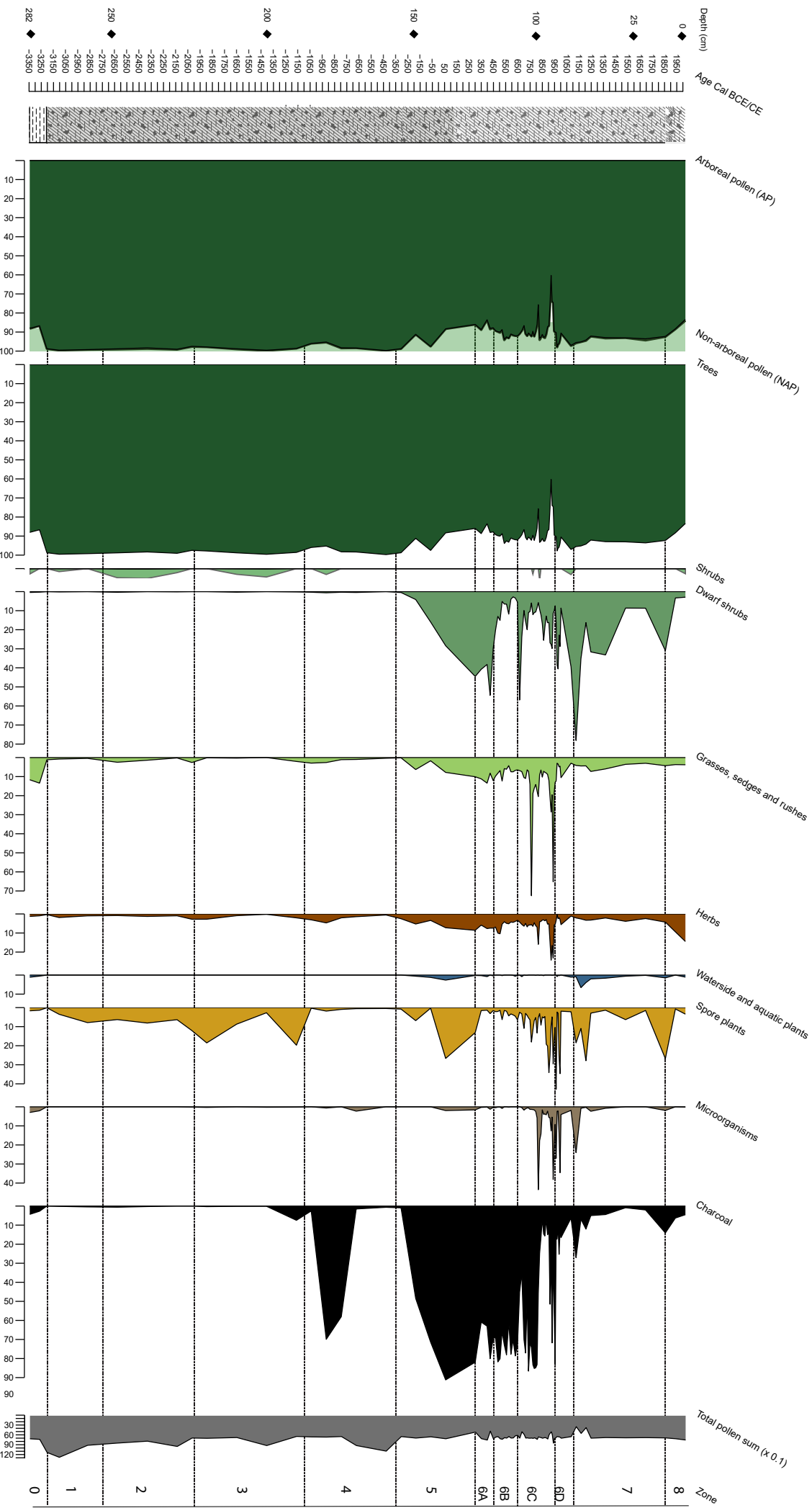
Appendix A.2: Part two of the percentage pollen diagram showing the entire pollen record of Haraldstadmyr peat sequence (see page 82 for the complete figure description).



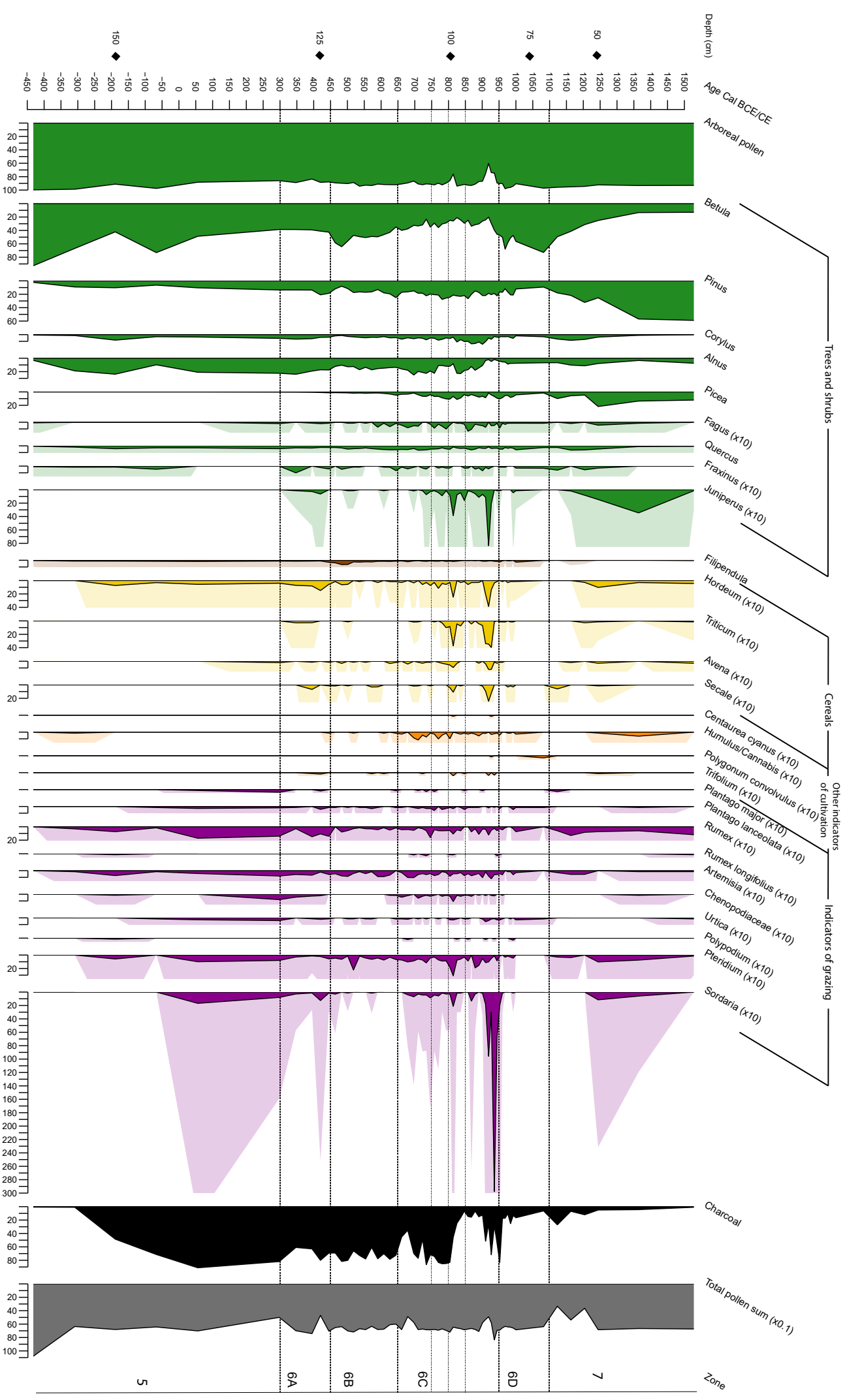
Appendix A.3: Part three of the percentage pollen diagram showing the entire pollen record of Haraldstadnyr peat sequence (see page 83 for the complete figure description).



Appendix A.4: Percentage pollen diagram showing the main pollen type categories of the entire pollen record of Haraldstadyr peat sequence (see page 83 for the complete figure description).



Appendix A.5: Selective percentage pollen diagram showing a selection of trees and shrubs, and the anthropogenic indicators of the pollen record of Haraldstadmyr peat sequence (see page 83 for the complete figure description).



Appendix B: The uncalibrated radiocarbon dates from Bjørnstad burial site (Iversen 2018).



LUNDS
UNIVERSITET

Geologiska Institutionen
Laboratoriet för ¹⁴C-datering
Sölvegatan 12, Geocentrum II
223 62 LUND
Tel. 046/2227856 Fax 046/2224830



Department of Geology
Radiocarbon Dating Laboratory
Sölvegatan 12, Geocentrum II
S-223 62 LUND
Sweden

Frode Iversen
Kulturhistorisk Museum, Universitetet i Oslo
Postboks 6762 St. Olavs plass, N-0130 Oslo, Norge

Dateringsattest

Provets benämning	Lab no	Erhållen ¹⁴ C-ålder BP	Provmgd (mg C)	Förbehandling
Bjørnstad s., Sarpsborg, Ostfold	P5001, A109 LuS 12917	1740 ± 40	1,5	NACIO, Hac
Bjørnstad s., Sarpsborg, Ostfold	P5002, A115 LuS 12918	1355 ± 40	1,4	NACIO, Hac
Bjørnstad s., Sarpsborg, Ostfold	P5003, A120 LuS 12919	1935 ± 45	0,6	NACIO, Hac
Bjørnstad s., Sarpsborg, Ostfold	P5004, A123 LuS 12920	1755 ± 40	0,9	NACIO, Hac
Bjørnstad s., Sarpsborg, Ostfold	P5005, A137 LuS 12921	1165 ± 40	0,6	NACIO, Hac
Bjørnstad s., Sarpsborg, Ostfold	P5006, A141 LuS 12922	1620 ± 40	1,1	NACIO, Hac
Bjørnstad s., Sarpsborg, Ostfold	P5007, A156 LuS 12923	1555 ± 40	1,1	NACIO, Hac
Bjørnstad s., Sarpsborg, Ostfold	P5008, A157 LuS 12924	1695 ± 40	0,9	NACIO, Hac
Bjørnstad s., Sarpsborg, Ostfold	P5020, A206 LuS 12925	1265 ± 40	1,2	NACIO, Hac
Bjørnstad s., Sarpsborg, Ostfold	P5032, A143 LuS 12926	1690 ± 45	0,4	NACIO, Hac
Bjørnstad s., Sarpsborg, Ostfold	P5049, A141 LuS 12927	1815 ± 45	0,4	NACIO, Hac
Bjørnstad s., Sarpsborg, Ostfold	P5050, A139 LuS 12928	1840 ± 45	0,5	NACIO, Hac

Bestämningen av ¹⁴C-åldern är baserad på halveringstiden 5568 år. Resultaten är givna i åtal ut före 1950 (¹⁴C-ålder BP). I osäkerhetsangivelsen inräknas misstänkt atmosfärisk förändring från utsläppen av kväve, standard och bakgrund. Som standard användes enligt internationell överenskommette 95% av aktiviteten hos NBS analysstandard. Alla ¹⁴C-åldern är ¹³C-korrigerade för avvikelser från internationellt standardvärde på ¹³C/¹²C-förhållande. Kal-14 åldern måste övervägas till kalibrerade kal-14 är ges om ut användning av IntCal13 (för terrestra prover) eller Marine13 (för marina prover). För ytterligare information hänvisas till Radiocarbon Vol 55, nr 4, 2013.

Lund 2018-02-19

Raimund Muscheler

Mats Rundgren



LUNDS
UNIVERSITET

Geologiska Institutionen
Laboratoriet för ¹⁴C-datering
Sölvegatan 12, Geocentrum II
223 62 LUND
Tel. 046/2227856 Fax 046/2224830



Department of Geology
Radiocarbon Dating Laboratory
Sölvegatan 12, Geocentrum II
S-223 62 LUND
Sweden

Frode Iversen
Kulturhistorisk Museum, Universitetet i Oslo
Postboks 6762 St. Olavs plass, N-0130 Oslo, Norge

Dateringsattest

Provets benämning	Lab no	Erhållen ¹⁴ C-ålder BP	Provmgd (mg C)	Förbehandling
Bjornstad s. Sarpsborg, Ostfold P5051. A260	LuS 12929	1645 ± 40	2,2	NACIO, Hac
Bjornstad s. Sarpsborg, Ostfold P5057. A115	LuS 12930	1665 ± 40	3,2	NACIO, Hac
Bjornstad s. Sarpsborg, Ostfold P5059. A133	LuS 12931	1740 ± 40	2,6	NACIO, Hac
Bjornstad s. Sarpsborg, Ostfold P5061. A123	LuS 12932	1685 ± 45	2,8	NACIO, Hac
Bjornstad s. Sarpsborg, Ostfold P5066. A262	LuS 12933	1550 ± 40	1,9	NACIO, Hac
Bjornstad s. Sarpsborg, Ostfold P5067. A156	LuS 12934	1500 ± 40	1,5	NACIO, Hac
Bjornstad s. Sarpsborg, Ostfold P5081. A271	LuS 12935	1735 ± 40	0,9	NACIO, Hac
Bjornstad s. Sarpsborg, Ostfold P5096. A272	LuS 12936	1685 ± 40	1,5	NACIO, Hac
Bjornstad s. Sarpsborg, Ostfold P5101. A157	LuS 12937	1650 ± 40	0,7	NACIO, Hac
Bjornstad s. Sarpsborg, Ostfold P5111. A157	LuS 12938	2045 ± 45	1,6	NACIO, Hac
Bjornstad s. Sarpsborg, Ostfold P5137. A218	LuS 12939	1990 ± 40	0,7	NACIO, Hac
Bjornstad s. Sarpsborg, Ostfold P5155. A279	LuS 12940	2055 ± 40	0,8	NACIO, Hac

Beräkningen av ¹⁴C-åldern är baserad på halveringstiden 5568 år. Resultaten är givna i antal år före 1950 (¹⁴C-ålder BP). I osäkerhetsangivelsen innefattas statistiskt oåtkomliga bidrag från mätningen av prov, standard och bakgrund. Som standard användes enligt internationell överenskommelse 95% av aktiviteten hos NBS oxalsyre-standard. Alla ¹⁴C-åldrar är ¹³C-korrigerade för avvikelsen från överenskommen standardvärde på ¹³C/¹²C-förhållandet. Kal-14 ålderna måste övervakas till kalibrerade kal-14 år genom att användas antingen IntCal13 (för terrestra prover) eller Marine13 (för marina prover). För ytterligare information hänvisas till Radiocarbon Vol 55, nr4, 2013.

Lund 2018-02-19

Raimund Muscheler

Mats Rundgren



LUNDS
UNIVERSITET

Geologiska Institutionen
Laboratoriet för ¹⁴C-datering
Sölvegatan 12, Geocentrum II
223 62 LUND
Tel. 046/2227856 Fax 046/2224830



Department of Geology
Radiocarbon Dating Laboratory
Sölvegatan 12, Geocentrum II
S-223 62 LUND
Sweden

Frode Iversen
Kulturhistorisk Museum, Universitetet i Oslo
Postboks 6762 St. Olavs plass, N-0130 Oslo, Norge

Dateringsattest

Provets benämning	Lab no	Erhållen ¹⁴ C-ålder BP	Provmgd (mg C)	Förbehandling
Bjornstad søndre, Sarpsborg P5026. A251	LuS 13368	2430 ± 40	1,7	HCl, NaOH
Bjornstad søndre, Sarpsborg P5030. A197A	LuS 13369	2475 ± 45	1,6	HCl, NaOH
Bjornstad søndre, Sarpsborg P5031. A197B	LuS 13370	2485 ± 40	1,6	HCl, NaOH
Bjornstad søndre, Sarpsborg P5033. A138	LuS 13371	1695 ± 40	1,6	HCl, NaOH
Bjornstad søndre, Sarpsborg P5035. A102	LuS 13372	1800 ± 40	1,6	HCl, NaOH
Bjornstad søndre, Sarpsborg P5040. A245	LuS 13373	190 ± 35	1,7	HCl, NaOH
Bjornstad søndre, Sarpsborg P5062. A179	LuS 13374	265 ± 35	1,6	HCl, NaOH
Bjornstad søndre, Sarpsborg P5065. A183	LuS 13375	915 ± 35	1,6	HCl, NaOH
Bjornstad søndre, Sarpsborg P5073. A263	LuS 13376	1585 ± 40	1,6	HCl, NaOH
Bjornstad søndre, Sarpsborg P5074. A182	LuS 13377	2400 ± 40	0,9	HCl, NaOH
Bjornstad søndre, Sarpsborg P5082. A180	LuS 13378	1535 ± 40	1,0	HCl, NaOH
Bjornstad søndre, Sarpsborg P5083. A162	LuS 13379	500 ± 35	1,6	HCl, NaOH

Beräkningen av ¹⁴C-åldern är baserad på halveringstiden 5568 år. Resultaten är gjorda i antal år före 1950 (¹⁴C-ålder BP). I osäkerhetsangivelsen innefattas statistiskt oförelämpliga bidrag från mätningen av prov, standard och bakgrund. Som standard användes enligt internationell överenskomst 95% av aktiviteten hos NBS oxalysyre-standard. Alla ¹⁴C-åldrar är ¹³C-korrigerade för avvikelser från överenskommen standardvärde på ¹³C/¹²C-förhållandet. Kol-14 åldern måste översättas till kalibrerade kol-14 år genom att använda antingen IntCal13 (för terrestra prover) eller Marine13 (för marina prover). För ytterligare information hänvisas till Radiocarbon Vol 55, nr4, 2013.

Lund 2018-04-27

Raimund Muscheler

Mats Rundgren



LUNDS
UNIVERSITET

Geologiska Institutionen
Laboratoriet för ¹⁴C-datering
Sölvegatan 12, Geocentrum II
223 62 LUND
Tel. 046/2227856 Fax 046/2224830



Department of Geology
Radiocarbon Dating Laboratory
Sölvegatan 12, Geocentrum II
S-223 62 LUND
Sweden

Frode Iversen
Kulturhistorisk Museum, Universitetet i Oslo
Postboks 6762 St. Olavsplass, N-0130 Oslo, Norge

Dateringsattest

Provets benämning	Lab no	Erhållen ¹⁴ C-ålder BP	Provmgd (mg C)	Förbehandling
Bjornstad søndre, Sarpsborg P5109. A176	LuS 13380	840 ± 35	1,4	HCl, NaOH
Bjornstad søndre, Sarpsborg P5113. A190	LuS 13381	840 ± 35	1,6	HCl, NaOH
Bjornstad søndre, Sarpsborg P5127. A125	LuS 13382	2490 ± 40	1,4	HCl, NaOH
Bjornstad søndre, Sarpsborg P5134. A149	LuS 13383	2445 ± 40	1,9	HCl, NaOH
Bjornstad søndre, Sarpsborg P5149. A212	LuS 13384	635 ± 35	1,4	HCl, NaOH
Bjornstad søndre, Sarpsborg P5150. A213	LuS 13385	255 ± 35	1,7	HCl, NaOH
Bjornstad søndre, Sarpsborg P5151. A214	LuS 13386	400 ± 40	1,4	HCl, NaOH

Beräkningen av ¹⁴C-åldern är baserad på halveringstiden 5568 år. Resultaten är givna i antal år före 1950 (¹⁴C-ålder BP). I osäkerhetsangivelsen innefattas statistiska åtkomliga bildning från mätningen av prov, standard och bakgrund. Som standard användes enligt internationell överenskommeelse 95% av aktiviteten hos NBS oxalsyre-standard. Alla ¹⁴C-åldrar är ¹³C-korrigerade för avvikelsen från överenskommen standardvärde på ¹³C/¹²C-förhållandet. ¹⁴C-åldern måste översättas till kalibrerade kal-14 år genom att använda utgången IntCal13 (för terrestra prover) eller Marine13 (för marina prover). För ytterligare information hänvisas till Radiocarbon Vol 55, nr 4, 2013.

Lund 2018-04-27

Raimund Muscheler

Mats Rundgren

Appendix C: New ¹⁴C radiocarbon dating in 2021

Due to the absence of radiocarbon dates on the deeper part of the core (123.5-282 cm), 4 new ¹⁴C bulk samples were sent in for radiocarbon dating. Even though the results were not available in time for this study, they were taken for future research on the bog. The samples were taken on the 10th of February 2021.

Whereas the previous radiocarbon samples were taken on the outer side of the core, these samples, except for sample HAR 18 ¼, were taken on the inner side of the core. In order to prevent contamination, a thin top layer of the inner side of the core was scraped off, before taking out approximately 1 cm³ of peat for each new sample. The samples were carefully placed in plastic sample bags. In between each sample the knife was cleaned in order to prevent contamination of the material. The samples were not sieved. During sampling, larger pieces of grass and branches across the core were avoided due to potential disturbance they can cause in the stratification, thereby disturbing the chronology of the core, which would result in an incorrect dating. Additionally, the sampling of aquatic plants was avoided, as they can contain significant amounts of carbon from the carbon cycle, and they usually grow locally in lakes or peat bogs. Both of these factors tend to cause unreliable ages.

Pictures of each sample were taken and the depths were accurately measured and noted down. Subsequently, the samples were scaled. Four forms were filled out including all necessary information for the samples taken, such as location of the site, position of the sample, type of material, type of core and coring equipment, estimated age and estimated weight. The radiocarbon samples and the forms were sent in to the *Lund University Radiocarbon Dating Laboratory*, located in Lund, Sweden.

The table below (Table 10) describes the extra samples taken for additional radiocarbon dating in order to improve the age-depth model in the future.

Table 10: Samples taken for radiocarbon dating in February 2021

Sample number	Core depth (cm)	Estimated age (cal. BP)	Weight (mg)
HAR18 1/4	20-21	258	514
HAR18 2/4	150-151	2139	942
HAR18 3/4	203-204	3434	1086
HAR18 4/4	275.5-277	5177	1183

Appendix D: The script used for plotting the pollen diagrams in 'R'.

```
#opening packages
library("ggplot2")
library("neotoma")
library("rioja")
library("tidyverse")

#setting directory where CSV file can be found
setwd("/Users/staples/Desktop/")

#reading CSV file
ma.pollen.raw <- read.csv("....csv", header=TRUE, sep=",",
check.names=FALSE)

#setting age as first column of the CSV file to use it in the plot as y-axis (y-var)
age <- ma.pollen.raw[,1]

#removing first column to remove the 'age' column in the pollen plot
ma.pollen1 <- ma.pollen.raw[,-1]

#defining the colour scheme
p.col <- c(rep("darkorange4", times=3), rep("steelblue4", times=8),
rep("goldenrod3", times=8), rep("navajowhite4", times=7), rep('goldenrod3',
times=1), rep("black", times=1))

#adding exaggeration
ex <- c(rep(TRUE, times=12), rep(FALSE, times=1), rep(TRUE, times=2),
rep(FALSE, times=1), rep(TRUE, times=11), rep(FALSE, times=1))

#plotting the pollen diagrams
{r, fig.width=15, fig.height=10}
pol.plot <- strat.plot(ma.pollen1,
yvar=age,
```

```
y.tks=seq(from=-3350, to=1950, by=50),
#y.tks=seq(from=0, to=280, by=10),
#y.tks=age,
y.rev=FALSE,
plot.symb=FALSE,
plot.line=TRUE,
plot.poly=TRUE,
plot.bar=FALSE,
col.bar="grey22",
col.poly=p.col,
symb.pch=18,
symb.cex=1,
col.symb="darkgrey",
col.poly.line="black",
lwd.poly=100,
scale.percent=TRUE,
min.width=0.2,
xSpace=0.01,
x.pc.lab=TRUE,
x.pc.omit0=TRUE,
las=2,
cex.xlabel=0.7,
cex.ylabel=0.6,
srt.xlabel=60,
cex.yaxis=0.6,
cex.axis=0.6,
exag=ex,
col.exag="auto",
exag.alpha = 0.2,
exag.mult=20,
ylabel="Age (CE)")
```

```
dev.print(pdf, "...pdf") # copies the plot to a the PDF file
```